Research Division
CONTROL DATA CORPORATION
Minneapolis, Minnesota 55440

FINAL REPORT
Contract NAS5-10171

STRATOSPHERIC CIRCULATION STUDIES

BASED ON TIROS VII 15-MICRON DATA

Prepared by:

A. D. Belmont
W. C. Shen
G. W. Nicholas

for

NATIONAL AERONAUTICS AND SPACE ADMINISTRATION
Goddard Space Flight Center
Glenn Dale Road
Greenbelt, Maryland 20771

2 June 1967

PREFACE

The purpose of this study has been to examine various features of the global stratospheric circulation, utilizing the TIROS VII 15-micron temperature data, especially with respect to stratospheric sudden warmings at high latitudes and the possible relation of tropical stratospheric anticyclones to them.

Before interpreting the 15-micron data it was considered necessary to gain experience in applying the data to synoptic analysis. Hence this final report consists of two separate and self-contained studies. The first contains the results of our statistical verification of the TIROS data with appropriate radiosonde data and the second paper is a study of the sudden warmings which occurred during the year 1963-1964, for which 15-micron data were available. As it is intended to publish these papers separately in scientific journals, each is here presented in a self-contained format with separate abstracts and figures grouped at the end of each paper:

Paper I: COMPARISON OF TIROS VII, 15-MICRON DATA WITH RADIOSONDE TEMPERATURES

Paper II: ANTARCTIC STRATOSPHERIC WARMINGS DURING 1963 REVEALED BY TIROS VII, 15-MICRON DATA

Research Division
CONTROL DATA CORPORATION
Minneapolis, Minnesota 55440

FINAL REPORT
Contract NAS5-10171

Paper I

COMPARISON OF TIROS VII, 15-MICRON DATA WITH RADIOSONDE TEMPERATURES

Prepared by:

A. D. Belmont
G. W. Nicholas
W. C. Shen

for

NATIONAL AERONAUTICS AND SPACE ADMINISTRATION
Goddard Space Flight Center
Glenn Dale Road
Greenbelt, Maryland 20771

2 June 1967

ABSTRACT

Temperatures derived from the 15-micron carbon dioxide channel of the radiometer carried aboard the TIROS VII satellite were compared to the radiosonde temperatures at 100, 70, 50, 30, 20 and 10 mb at 97 stations in the northern hemisphere from 20 January to 17 February 1964. The 15-micron temperature is rarely colder than the 30-mb temperature, and it generally falls between the 10- and 30-mb temperature. The highest correlation between 15-micron and radiosonde temperatures was 0.7 at both 30 mb and 20 mb, near the level of maximum weight which applies to the 15-micron radiance weighting function profile.

TABLE OF CONTENTS

LIST OF FIGURES

LIST OF FIGURES
(cont'd)

I. Introduction

Extensive observation of temperature in the stratosphere on a quasi-global scale began with the launch of the TIROS VII satellite on June 19, 1963. One of the five channels of the radiometer carried aboard the satellite measured the thermal radiation at wavelengths ranging from 14.8 to 15.5 microns which is strongly emitted by carbon dioxide. As the temperature of the carbon dioxide can be assumed to be the same as the air in which it is located, the intensities can be interpreted in terms of a weighted-mean, equivalent blackbody temperature over the mid- and lower stratosphere. Radiative transfer theory shows that the radiation in this spectral range is mainly emitted in the region from 15 to 35 km (Nordberg et al, 1965). The maximum contribution at low nadir angles generally originates at about 23-25 km. The 15-micron temperature[1] corresponds to different heights from day-to-day, as the temperature at various levels changes. However, as the pressure surfaces vary in phase with the temperature (i.e. rise when temperature increases), there is reason to expect better correlation of 15-micron temperature with constant pressure than with constant height surfaces.

According to Nordberg (1966) cloudiness below 5 km does not affect the 15-micron temperatures, but radiation from thick high clouds, such as over large thunderstorms, may cause 15-micron temperature decreases of 5 to 10C. Clouds raise the peak of the weighting function profile which means the effective 15-micron temperature represents a higher layer in the atmosphere than without the cloud layer. In this limited study, however, the effect of cloudiness could not be considered.

[1] In this report the temperatures derived from the 15-micron channel radiation intensities will be referred to as 15-micron temperatures.

The TIROS VII orbits were nearly circular with a mean height of 635 km. The aperture angle of the radiometer was approximately five degrees; thus, the instantaneous area viewed on the earth's surface when the radiometer was directed straight down was a circular spot of about 55 km in diameter. The inclination of the orbital plane was 58° resulting in data coverage to about 60N and 60S when the nadir viewing angles were restricted to the range from 0° to 40°. Readings were taken at the rate of 16 per second. This method of obtaining quasi-global temperatures is potentially a very useful means for studying stratospheric phenomena both synoptically and climatologically. Nordberg et al (1965), Warnecke (1966), and Teweles (1966) have demonstrated that the 15-micron temperature pattern can reflect certain large-scale thermal events in both space and time in the middle and lower stratosphere.

However, because the 15-micron temperatures are weighted mean temperatures over an indefinite height range in the stratosphere, the question which the stratospheric meteorologist raises is "which pressure level or height do these temperatures really represent, or can one, in fact, interpret them at all in terms of temperature at a single pressure level or height?" The purpose of this report is to compare the 15-micron temperatures with radiosonde data to determine at which pressure level there is optimum correspondence.

II. Data

The 15-micron channel of the TIROS VII medium resolution radiometer changed in response after going into orbit, as did all channels of previous instruments flown on TIROS satellites. Soon after launch it became apparent that a different type of deviation from the original preflight calibration had occurred in the 15-micron channel in addition to the deviations experienced from previous satellites. The radiometer which alternatingly views the earth through either the floor or wall of the satellite showed that a consistently lower response occurred on the wall side when both viewed the same general target within a few minutes. Although the cause of this floor-wall difference can not be explained fully, the amount and its pattern has been determined allowing corrections to be made to the data. All of the 15-micron data used in this report were corrected by the method reported by Staff Members (1965). Even after corrections are applied, there are some uncertainties in the absolute and relative magnitudes of the derived temperatures. These uncertainties, however, are believed to be small, especially in the relative magnitudes over short periods of time; and the implications drawn from the distribution of the temperature patterns are not appreciably affected.

The 15-micron channel data were characterized also by random noise of an RMS amplitude of about 5C due to a small signal-to-noise ratio (Kennedy, 1966). The data in this report were not filtered to eliminate the short wave perturbations due to this noise component. Spatial averaging of the observations and smoothing of the map analysis reduced the noise component to a large extent.

The TIROS data were subjected to two other important restrictions. First, to avoid gross mislocation of the data by the computer, it was instructed to reject all scans with minimum nadir angles greater than 38° occurring within the scan. This restriction eliminated most of the alternating open mode and closed mode data and retained only the open mode data that can be accurately located by the computer. Second, the computer was instructed to reject all individual measurements within a scan with nadir angles greater than 40° to minimize the effect of shifting the height of the peak emission in the 15-micron region upward. When the data were mapped, these two restrictions, plus the orbital geometry, produced several gaps in the coverage.

The sampling rate of the radiation data was chosen to permit overlapping of one-half for successive scan spots each of which is at least 55 km in diameter. The geographic coordinates for the center of each scan spot are determined. When the data are mapped, the computer averages all of individual values that are located within a rectangular area. For the 1 to 40 million Mercator map used to map the 15-micron temperatures in this report, the size of the rectangular area was constant at 5 degrees of longitude in the zonal direction and variable in the meridional direction, ranging from 5 degrees at the equator to approximately 2.5 degrees at 60 degrees latitude. As a result each grid-point temperature represented an average of up to about 200 individual observations. If a grid-point average resulted from 10 or less single observations, the value was not included in the isothermal analysis.

TIROS data for individual orbits, observed within about 12 hours of the radiosonde observation time (1200 GMT) were plotted on daily maps. The

orbits for this period generally happened to occur on a single calendar day. At the beginning of the period these orbits usually occurred from 0 to 12 hours after the map reference time and with each succeeding day this 12 hour period occurred earlier so that by the last day 17 February, the 8 daily orbits were almost centered around the noon reference time. Isotherms were drawn to produce a 15-micron thermal field which was smoothed over a 12 hour period and extrapolated across data gaps. From the 24 analyzed maps which had reasonable coverage during the period 20 January through 17 February, 1964, values of the smoothed 15-micron isotherms were read at locations for which radiosonde temperatures were also available.

The best available comparative radiosonde data were those used for the daily northern hemisphere stratospheric map series prepared by the Environmental Science Services Administration. Temperatures were extracted at 97 stations over North America and Europe and the values at 100, 70, 50, 30, 20 and 10 mb taken at 1200 GMT were used in this study. These radiosonde temperatures were corrected for radiation by the method given by Finger et al (1965).

III. Results

a. Correlations

Warnecke (1966) found a high correlation between the 30-mb and the 15-micron temperatures. Using preliminary, uncorrected 15-micron data for one day, his findings showed correlation coefficients of 0.90 for 247 values in the northern hemisphere and 0.94 for 234 values in the southern hemisphere. His scatter diagrams showed that the temperatures were distributed parallel to a line through the origin with a slope of one indicating that the 15-micron temperature was systematically warmer than the 30-mb temperature by 11.0C and 5.1C for the northern and southern hemispheres, respectively. After his comparison was made, factors were derived by Staff Members (1965) to correct the 15-micron temperatures for instrumental degradation.

Using corrected 15-micron data and radiosonde data from 97 northern hemisphere stations for 24 days from 20 January through 17 February 1964, correlations were computed between the 15-micron temperatures and the temperatures at six pressure levels from 100 to 10 mb. Data for 31 January and 9 through 12 February were not used because the 15-micron temperature coverage was too sparse to permit an isotherm analysis. The resulting coefficients are given in Table 1. The 20 and 30 mb levels show the highest coefficients of 0.71 and 0.72, respectively. The mean radiosonde temperature naturally varies greatly from level to level, and its standard deviation varies slightly, while the 15-micron means and deviations vary only with sample size. The maximum correlations occur at levels of minimum variability of the radiosonde temperatures. The difference between

the average 30-mb and the average 15-micron temperature is -8.6C; whereas the difference is only -6.5C at 20 mb although the correlations are nearly equal. At 10 mb the average temperatures are almost equal, but the standard deviation is greater and the correlation less.

The correlation coefficients were plotted as a function of height and compared to the weighting function which applies to the 15-micron outgoing radiance (Figure 1). Only the weighting functions for the tropical and the high latitude winter-cold atmosphere are shown as these curves represent the upper and lower limits of the peak weights. Note the similarity of the shape of the curves. The height of the maximum correlation, approximately 25 km, is very near the heights of the maximum 15-micron weights, between 20 and 25 km. A slight over-correction of the 15-micron temperatures could easily result in this small difference in height of the maximum correlation and maximum weight. This adds confidence, however, that the 15-micron temperature should be more representative of the 20 to 30 mb temperatures than temperatures at other levels.

Scatter diagrams of the 20-and 30-mb temperatures versus the 15-micron temperature were plotted (Fig. 2a, b) using the total population of 1078 and 1229 points, respectively. These diagrams are presented to demonstrate that it would be difficult to conclude that there is a systematic difference between the radiosonde and the 15-micron temperature at either level. Although there is considerable scatter, one can see that the two temperatures are more nearly the same at high values but the difference becomes progressively greater for lower values. Nordberg (1966) has shown by radiative

transfer theory that the 15-micron temperatures will change by varying amounts depending upon where the actual temperature changes occurs in relation to the weighting functions (Fig. 1b). Thus, one would not expect a one-to-one correspondence between the radiosonde temperature changes at any level and the 15-micron temperature change.

b. Time cross-sections

Time cross-sections of radiosonde temperatures between 100 and 10 mb were plotted for 19 stations varying in latitude from 16N to 52N. Only three are shown here in Figs. 3a, b and c. Each section covered 8 days from 24 through 31 January 1964. On these sections, the height corresponding to the 15-micron temperature for that location was marked. These sections show that the 15-micron temperatures correspond to the radiosonde temperatures that fall between the 10- and 30-mb level, and not lower than the 30-mb level.

It is also interesting to note that the 15-micron temperature follows the trend of the radiosonde temperature as a function of time. The sudden warming in the stratosphere reported by Nordberg (1965) that occurred over the Caspian Sea (Fig. 3a) shows that the 15-micron temperature increases as the radiosonde temperature changes in the 10 to 30 mb range. However, the 15-micron values increase less than the radiosonde temperatures, as would be expected considering the vertical and horizontal averaging represented by the former.

c. Longitudinal comparison of radiosonde and 15-micron temperatures

To further illustrate that the 15-micron temperature pattern corresponds to and changes as the radiosonde temperature pattern, the 10-mb, 30-mb, and 15-micron temperatures were plotted as a function of longitude for the 60N, 50N, and 40N latitude circles (Fig. 4) for 27 January 1964 when there was a strong longitudinal temperature gradient at these latitudes. The 15-micron temperature curve is seen to follow the same general trend as both the 10- and 30-mb temperature curve in all cases. In addition, the phase of the 15-micron temperature curve is more nearly in phase with the 30- than the 10-mb temperature curve, although the magnitude of the 15-micron temperatures correspond better to the 10-mb temperature. The amplitude of the 15-micron temperature curve is from 70 to 100 per cent of the 30-mb temperature curve, whereas, it is only 70 to 80 per cent of the 10-mb temperature curve.

The important points to be made from Fig. 4 are that (1) the 15-micron temperatures are capable of detecting stratosphere temperature changes, (2) the 15-micron temperatures are seldom colder than the 30-mb temperatures and generally fall between the 10- and 30-mb temperatures, and (3) the phase and amplitude of the 15-micron temperature curves are more nearly coincident with the 30- than the 10-mb temperature curve. From theory one would not expect the amplitude of the 15-micron temperature curve to be exactly the same as either of the radiosonde temperature curves; but it is significant that the phase and amplitude correspond better at 30 mb as this is nearer the height of maximum 15-micron emission.

d. Longitudinal comparison of the 10- and 30-mb heights with the 15-micron temperatures

The heights of the 10- and 30-mb surfaces and the 15-micron temperatures were plotted as a function of longitude (Fig. 5) to determine the relationship between pressure changes and the vertical mean temperature represented by the 15-micron temperature. There is a good relationship; where the 10- and 30-mb pressure surfaces are high the 15-micron temperature is high, and vice versa. However, the 15-micron temperature minimum lags by about 40° to 60° of longitude west of the height curves in all cases.

e. Longitudinal comparison of thickness and the 15-micron temperatures

The next obvious question is "how well do the 15-micron temperatures correspond to the thickness between two pressure levels at heights near the maximum 15-micron radiance?" The thickness between 100 and 10 mb and the 15-micron temperature were plotted as before as a function of longitude (Fig. 6). In all cases there is good agreement in the phase of the two curves which is better than the previous relationship with height curves. A comparison of the amplitudes is not possible as the units are different. It would seem possible that one could obtain thickness patterns from the 15-micron temperatures and by graphical addition to the contour pattern of a lower level obtain a contour pattern at a higher level. This constitutes a study of its own and will not be persued in this report.

An attempt was also made to determine if the 15-micron temperatures were better correlated to warm high-pressure systems and cold low-pressure

systems than to the total population. The radiosonde temperatures for each of the six pressure levels were divided into 16 groups by first selecting four height intervals and subdividing these height intervals into four temperature intervals. No systematic pattern could be found in the correlation for these 16 classes that would indicate that warm highs or cold lows were better correlated to the 15-micron temperatures than the population as a whole. However, this inconsistency may be due to the small sample size of each group, and should be tested with a larger population.

IV. Summary

The 15-micron temperature is a weighted mean temperature over an indefinite height range of the middle and lower stratosphere. Temperatures between 20 and 25 km are weighted most heavily with very little contribution coming from below 10 or above 35 km. Correlation coefficients between 15-micron temperatures and the temperatures at 6 pressure levels between 100 and 10 mb show that the highest correlations of .72 and .71 occur at levels of maximum 15-micron temperature weights; i.e., 30 and 20 mb with an average temperature difference of about 8 or 6C, respectively. The 15-micron temperature is seldom colder than the 30-mb temperature, and it generally falls between the 10- and 30-mb temperature. Plots of the 10-mb, 30-mb, and 15-micron temperatures versus longitude, along three high latitudes, show that the phase and amplitude of the 15-micron temperature curve is more nearly coincident with the 30-mb than the 10-mb temperature curve.

The evidence presented here indicate that the 15-micron temperatures correspond better to the 20 and 30 mb temperatures than any of the other commonly plotted pressure levels in the middle and lower stratosphere. One should use caution in interpreting the 15-micron temperatures as an equivalent of the 20 or 30 mb temperatures, however, as no evidence can be found of a systematic difference between the satellite and radiosonde values, nor should there be. The 15-micron temperature will change by varying amounts depending upon where the actual temperature change occurs in relation to the weighting function, although the 15-micron temperature change is more sensitive to the actual temperature change at the height where the radiance weighting function has its maximum.

V. References

Finger, F. G., H. M. Woolf and C. E. Anderson, 1965: A method for objective analysis of stratospheric constant-pressure charts. Monthly Weather Review, 93, 619-638.

Kennedy, J. S., 1966: An Atlas of Stratospheric Mean Isotherms Derived from TIROS VII Observations. GSFC document X-622-66-307, 85 pp. (Available from NASA, Goddard Space Flight Center, Greenbelt, Maryland).

Nordberg, W., W. R. Bandeen, G. Warnecke and V. Kunds, 1965: Stratospheric temperature patterns based on radiometric measurements from the TIROS VII satellite. Space Research V, Proceedings of the Fifth International Space Science Symposium, Florence, May 8-20, 1964, Amsterdam, North Holland Publishing Company, 783-809.

Nordberg, W., 1966: Satellite radiation measurements in spectral regions. In: Satellite Data in Meteorological Research, NCAR-TN-11, Boulder, Colorado, NCAR, 199-213.

Staff Members, 1965: TIROS VII Radiation Data Catalog and Users' Manual, Vol. 3, Greenbelt, Maryland, National Space Science Data Center, Goddard Space Flight Center, Code 601, 269 pp.

Teweles, S., 1966: Radiometer data in the 15μ band. In: Satellite Data in Meteorological Research, NCAR-TN-11, Boulder, Colorado, NCAR, 215-257.

References (cont'd)

Warnecke, G., 1966: TIROS VII 15μ radiometric measurements and mid-stratospheric temperatures. In: Satellite Data in Meteorological Research, NCAR-TN-11, Boulder, Colorado, NCAR, 215-227.

Table 1 Correlation coefficients between radiosonde temperatures and 15-micron temperatures at 97 stations for 24 days

Pressure Level	Correlation Coefficient	Average Radiosonde Temperature	Average 15-micron Temperature	Standard Deviation of the Radiosonde Temperature	Standard Deviation of the 15-micron Temperature	Sample Size
100	.33	-61.6	-48.1	10.02	5.08	1379
70	.35	-63.8	-48.3	8.93	4.94	910
50	.46	-59.0	-48.0	9.13	5.24	1384
30	.72	-56.7	-48.1	7.21	5.23	1229
20	.71	-54.4	-47.9	7.41	5.14	1078
10	.61	-48.0	-47.9	9.06	5.02	840

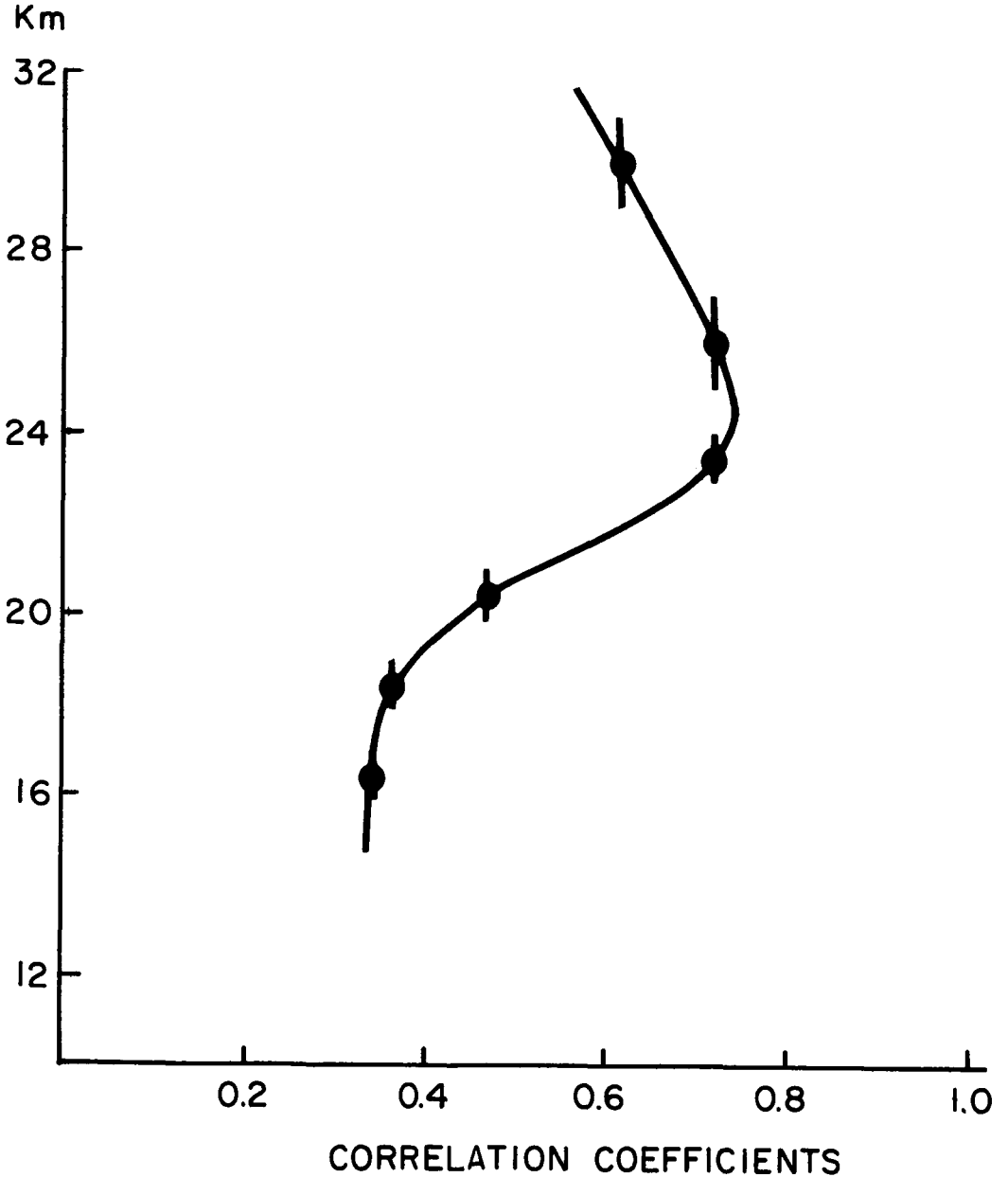

Figure 1a Correlation coefficients between the 15-micron temperatures and the radiosonde temperatures for six pressure levels from 100 to 10 mb plotted at the mid-point of the height range for each pressure level

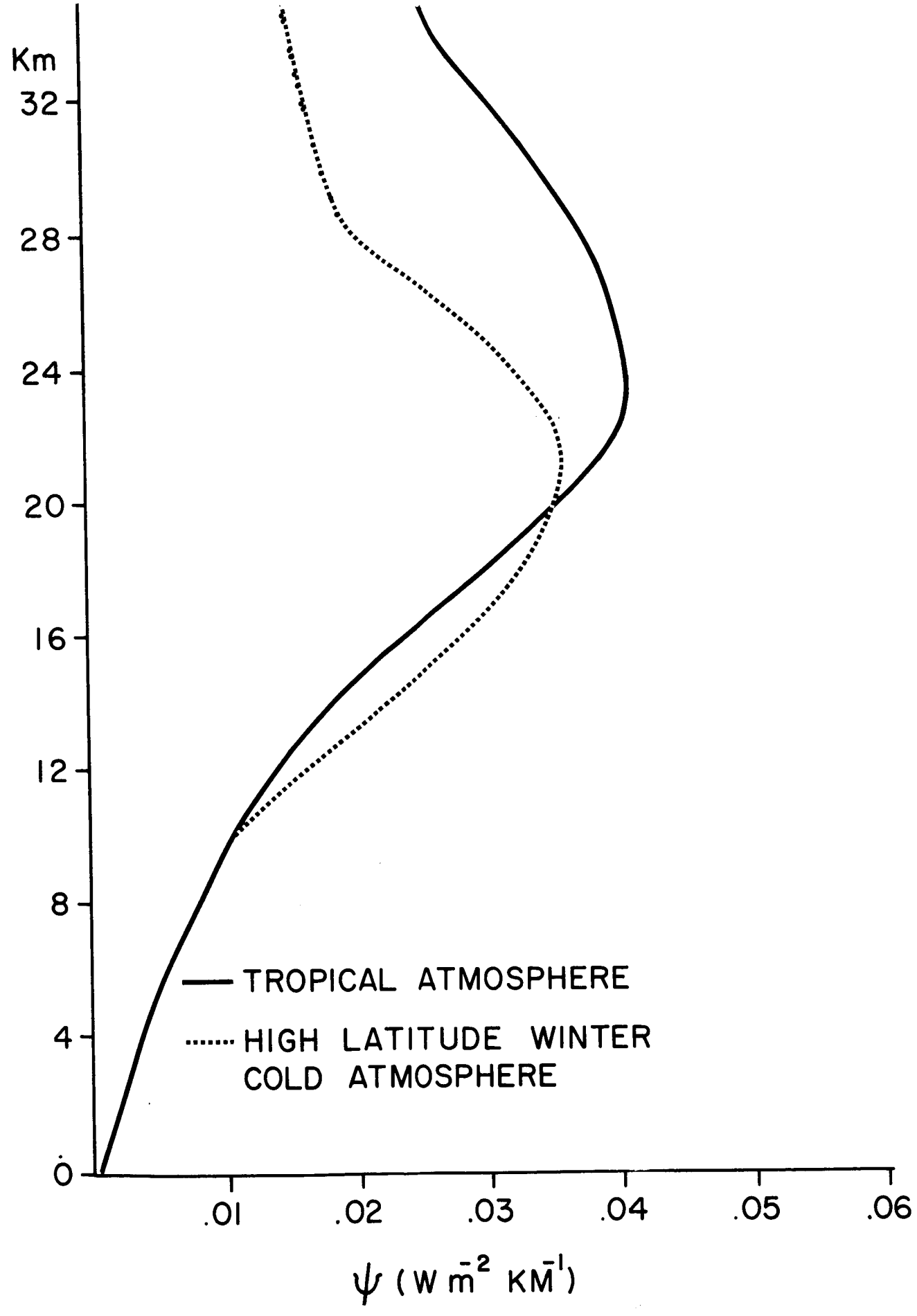

Figure 1b Weighting function applying to the measured outgoing radiance of the 15-micron channel at a nadir angle of zero after Nordberg, et al (1965)

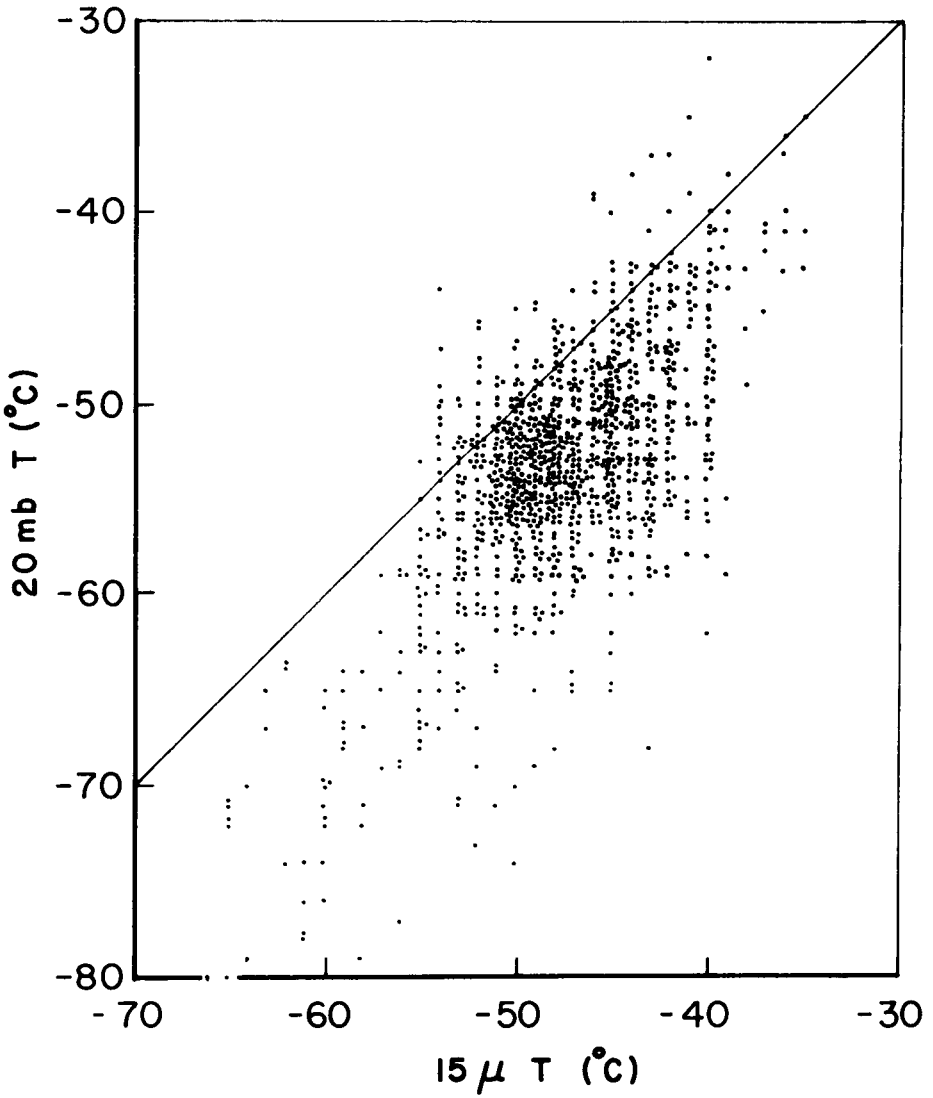

Figure 2a Scatter diagrams of the radiosonde 20-mb temperatures versus the 15-micron temperatures at 97 stations in the northern hemisphere for 24 days from 20 January through 17 February 1964

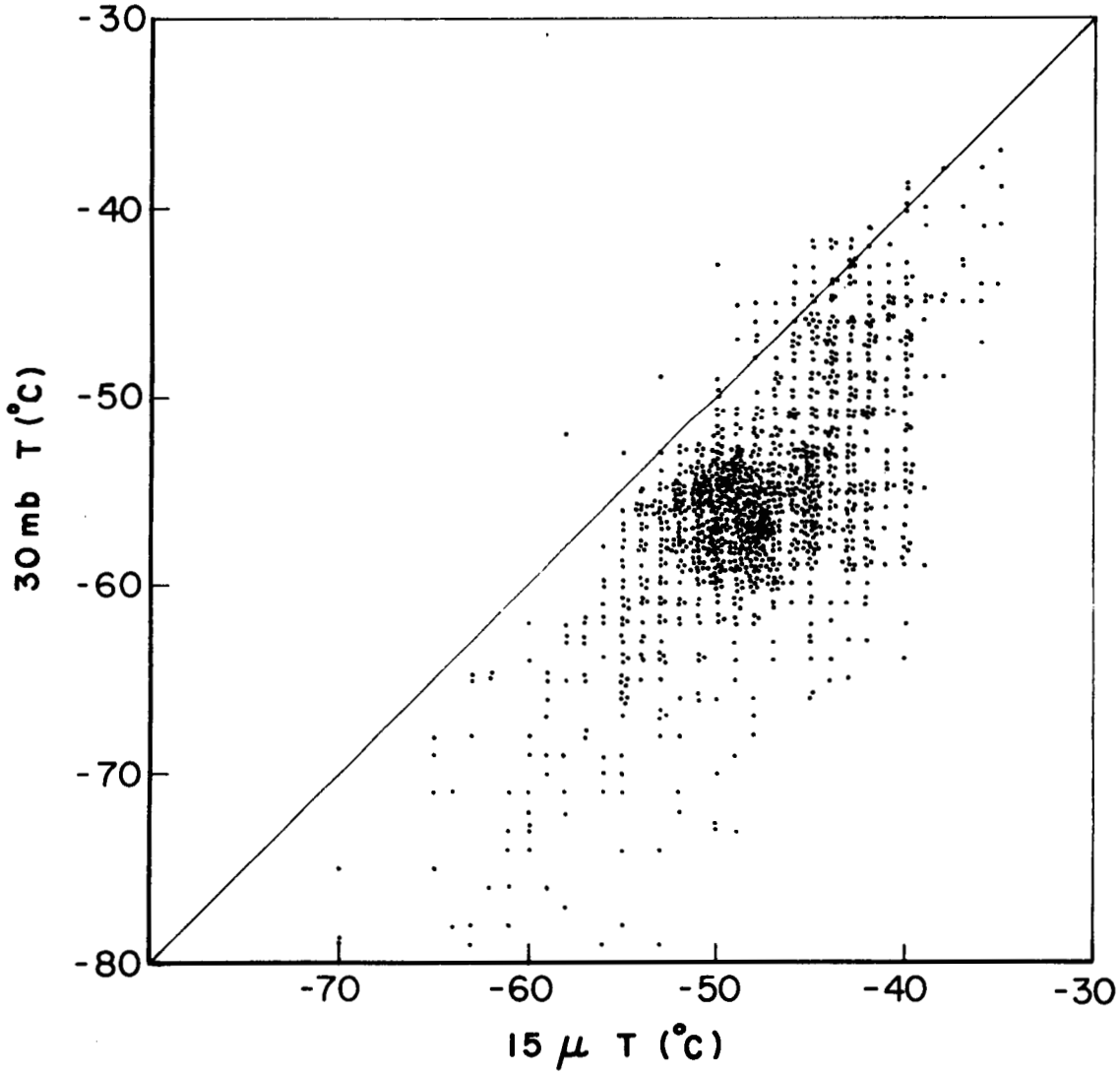

Figure 2b Scatter diagrams of the radiosonde 30-mb temperatures versus the 15-micron temperatures at 97 stations in the northern hemisphere for 24 days from 20 January through 17 February 1964

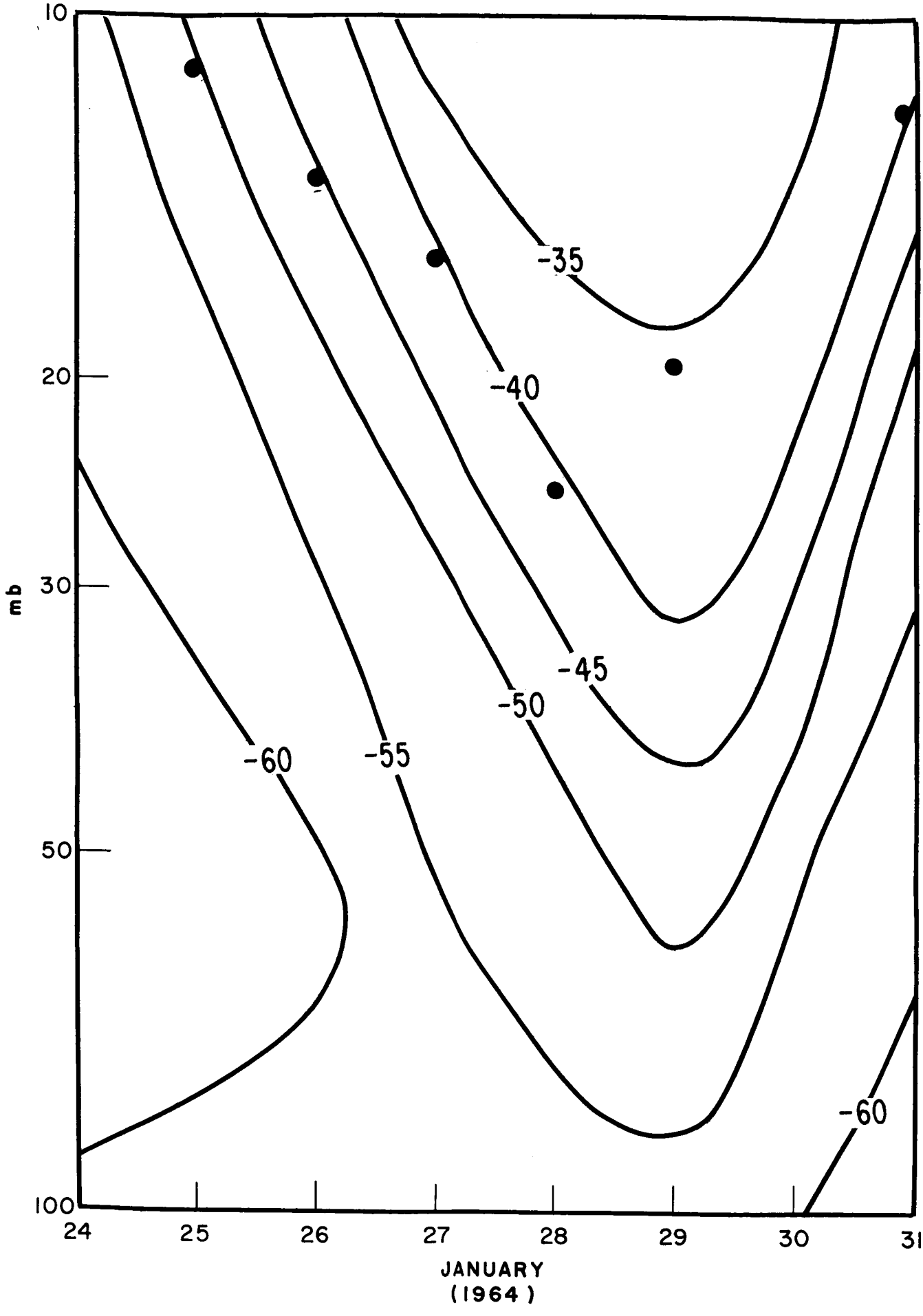

Figure 3a Time-height section of radiosonde temperature for Orenburg (52N, 55E) for the period from 24 through 31 January 1964. 15-micron temperatures are plotted at heights corresponding to the same radiosonde temperature

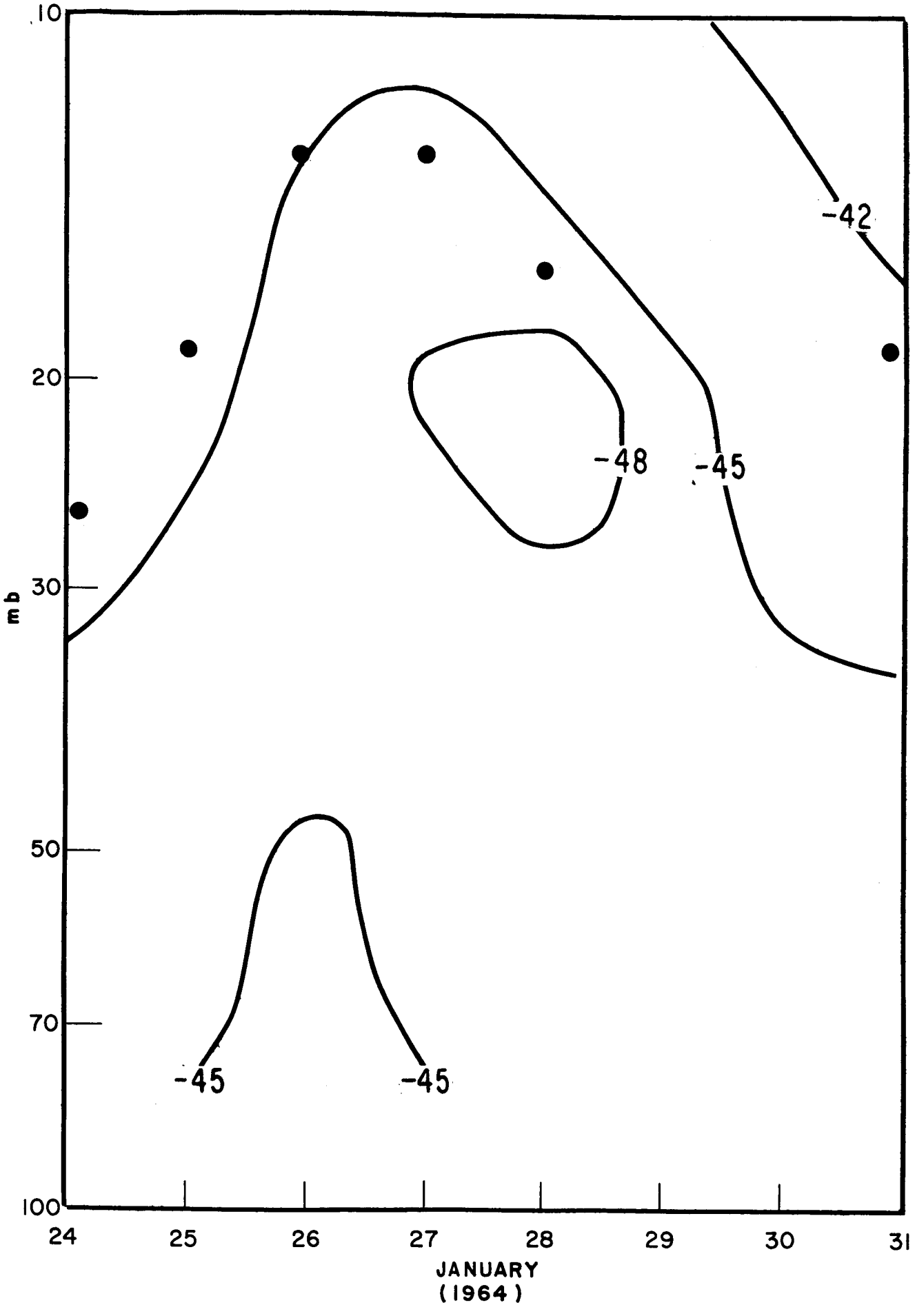

Figure 3b Time-height section of radiosonde temperature for B. Elan (47N, 143E) for the period from 24 through 31 January 1964. 15-micron temperatures are plotted at heights corresponding to the same radiosonde temperature

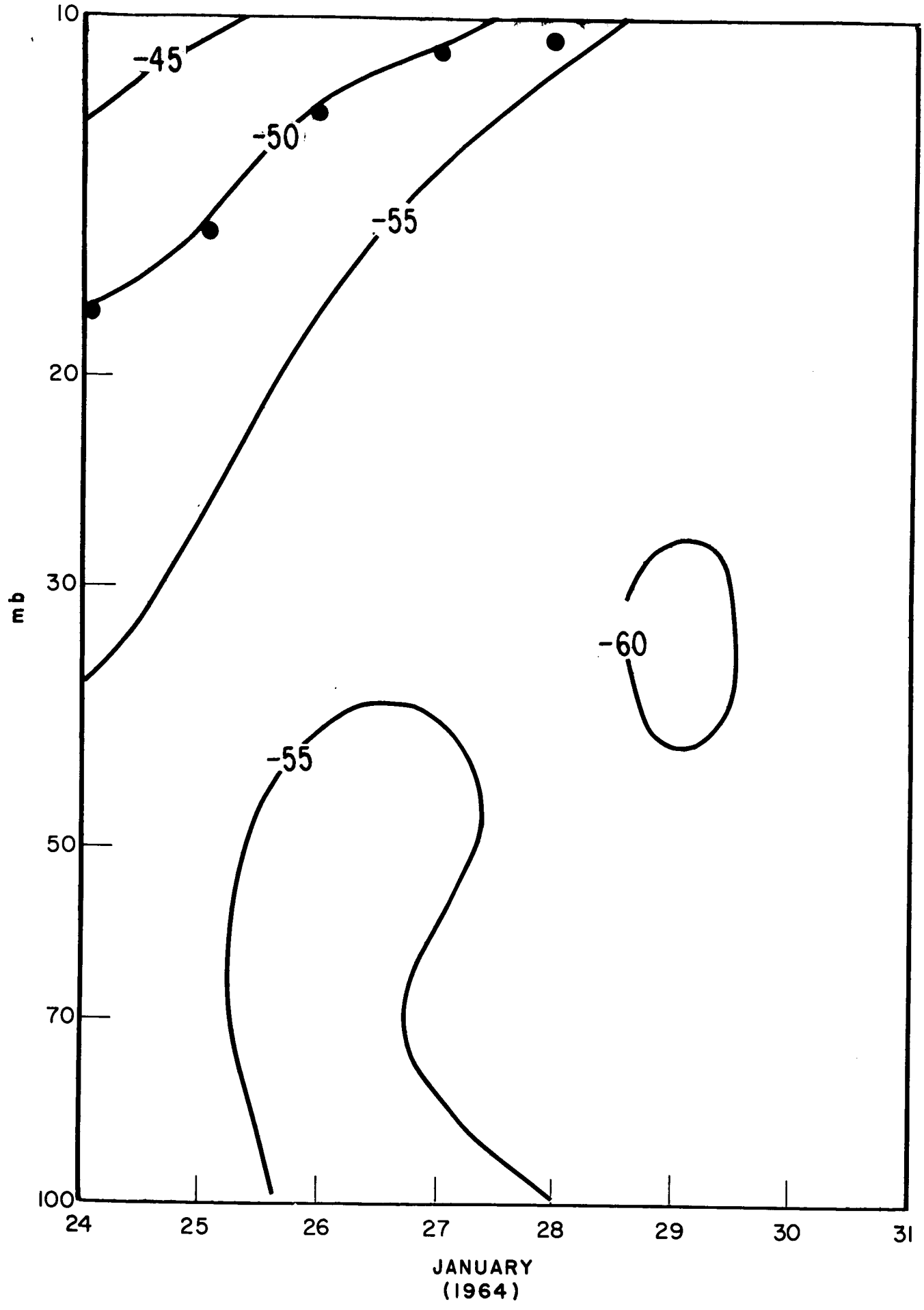

Figure 3c Time-height section of radiosonde temperature for S. Ste. Marie (46N, 84W) for the period from 24 through 31 January 1964. 15-micron temperatures are plotted at heights corresponding to the same radiosonde temperature

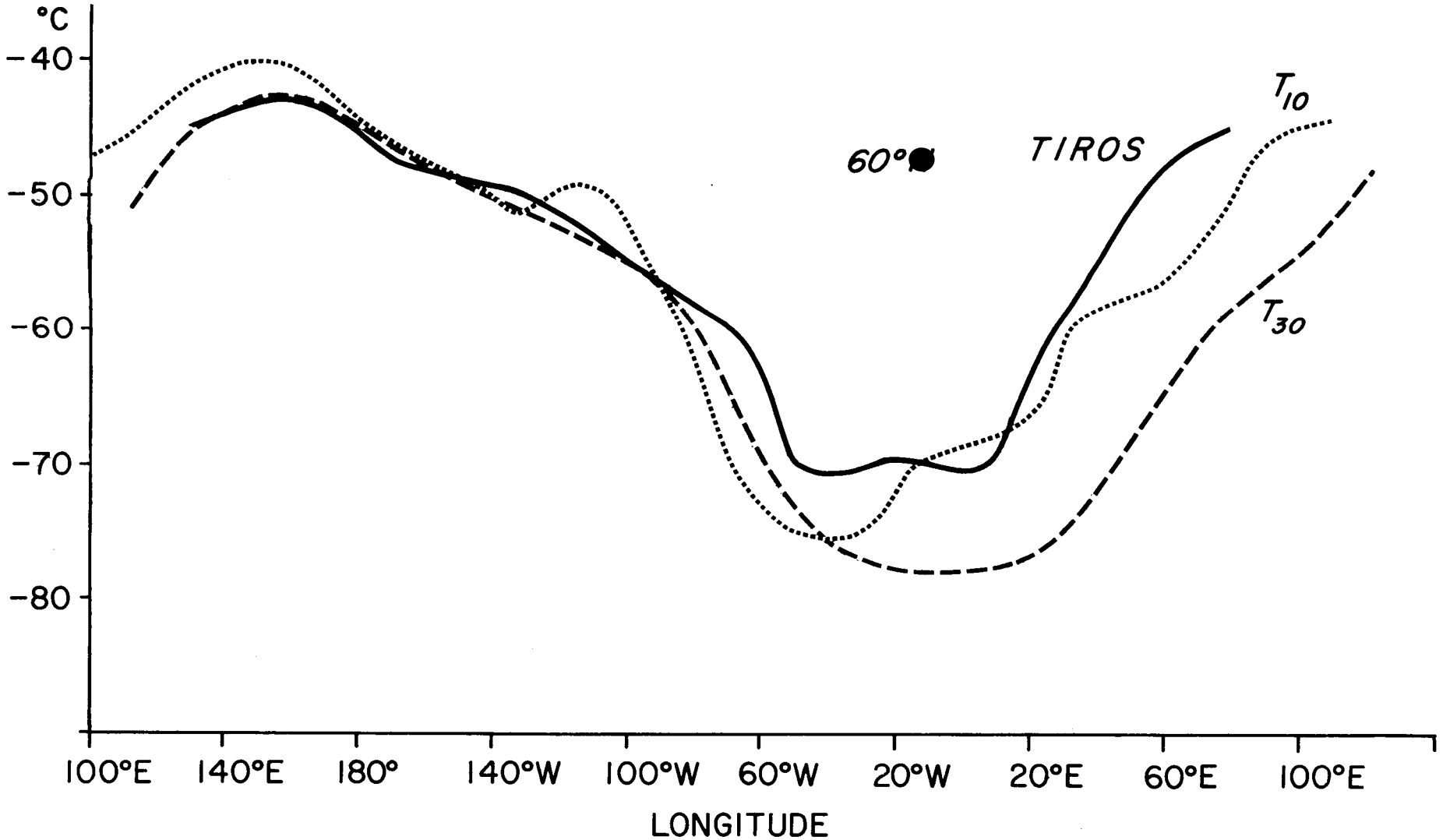

Figure 4a 30-mb, 10-mb, and 15-micron temperatures versus longitude at 60N, for 27 January 1964

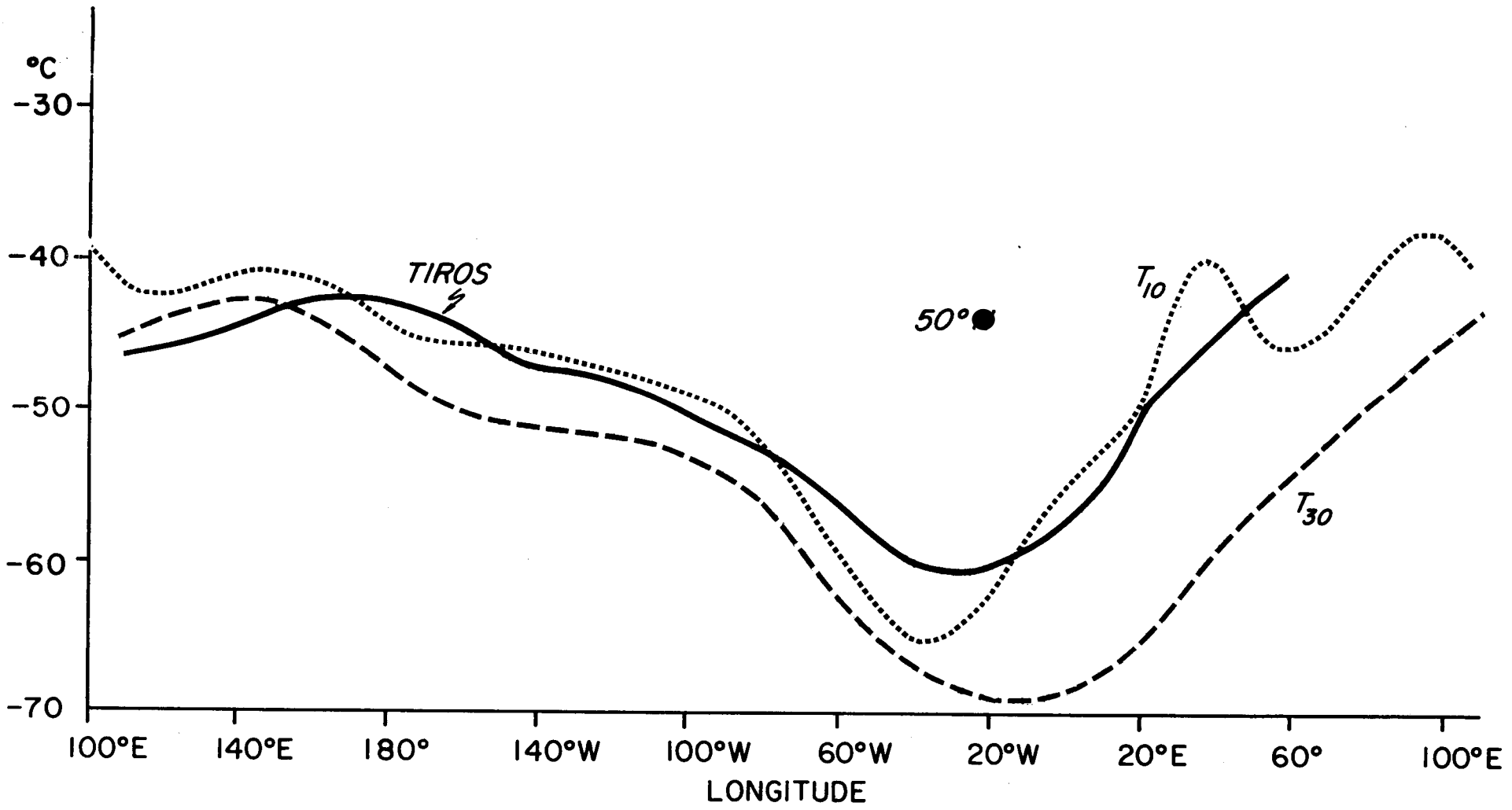

Figure 4b 30-mb, 10-mb, and 15-micron temperatures versus longitude at 50N, for 27 January 1964

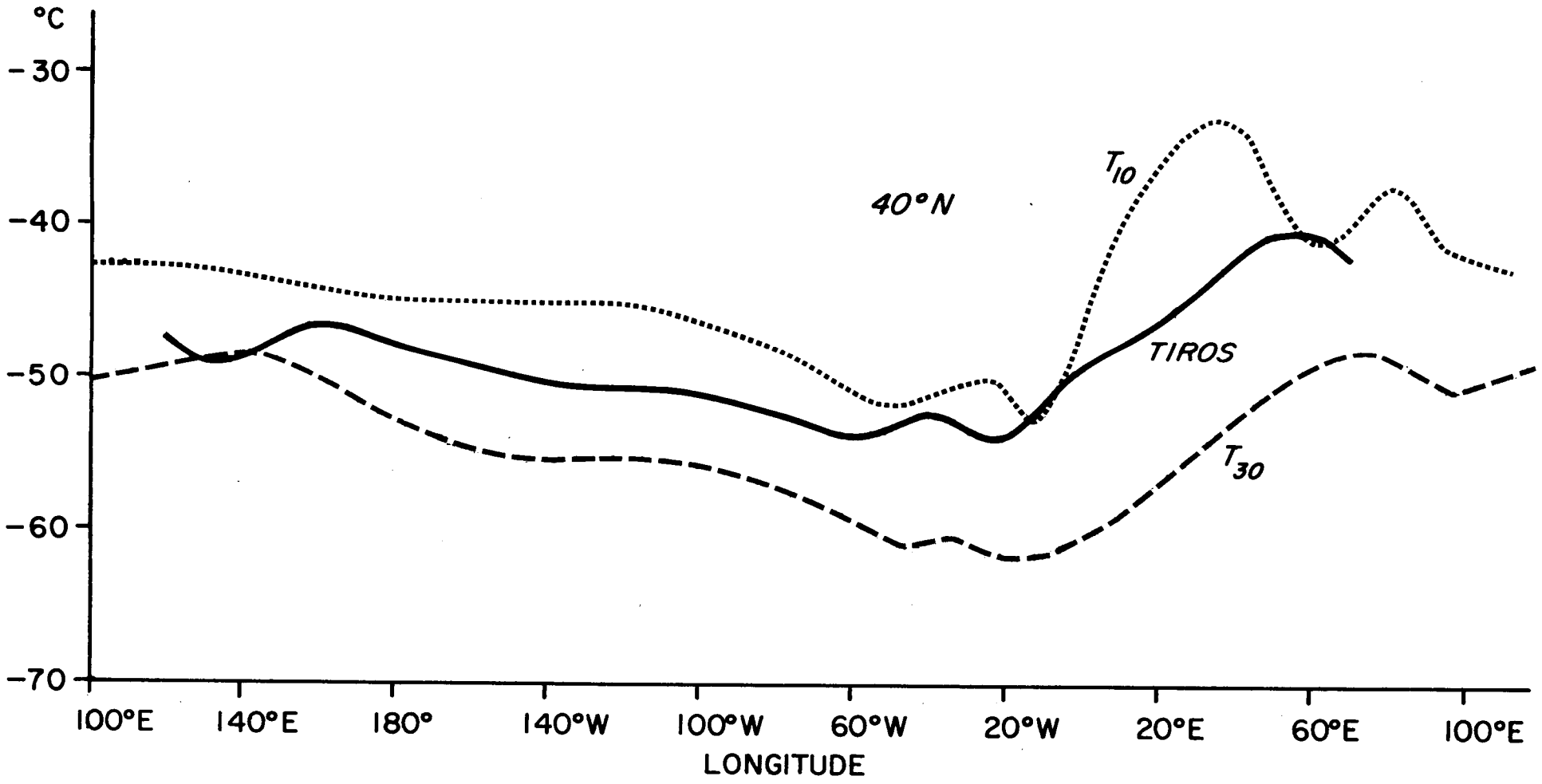

Figure 4c 30-mb, 10-mb, and 15-micron temperatures versus longitude at 40N, for 27 January 1964

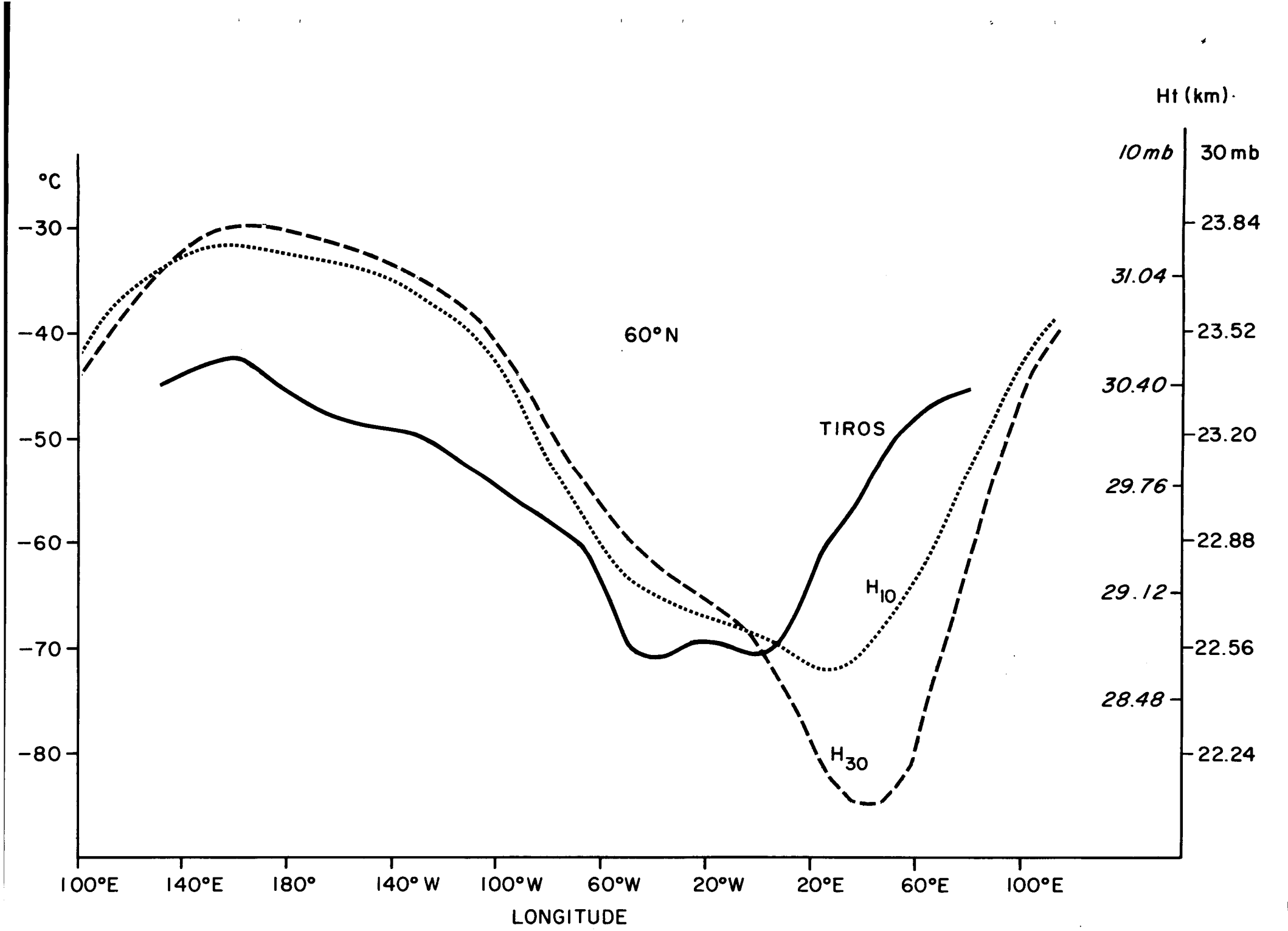

Figure 5a 30-mb and 10-mb heights and 15-micron temperature versus longitude at 60N, for 27 January 1964

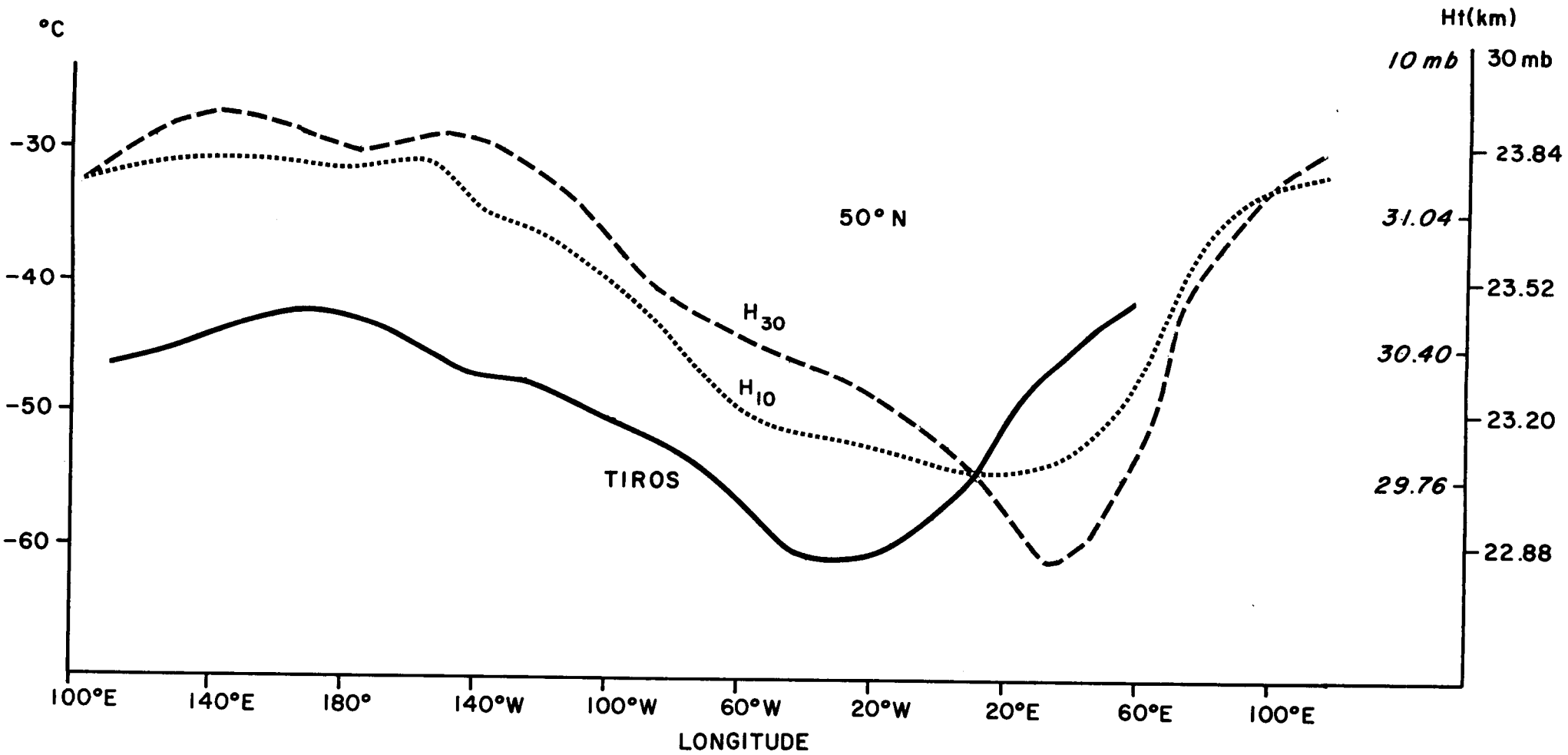

Figure 5b 30-mb and 10-mb heights and 15-micron temperature versus longitude at 50N, for 27 January 1964

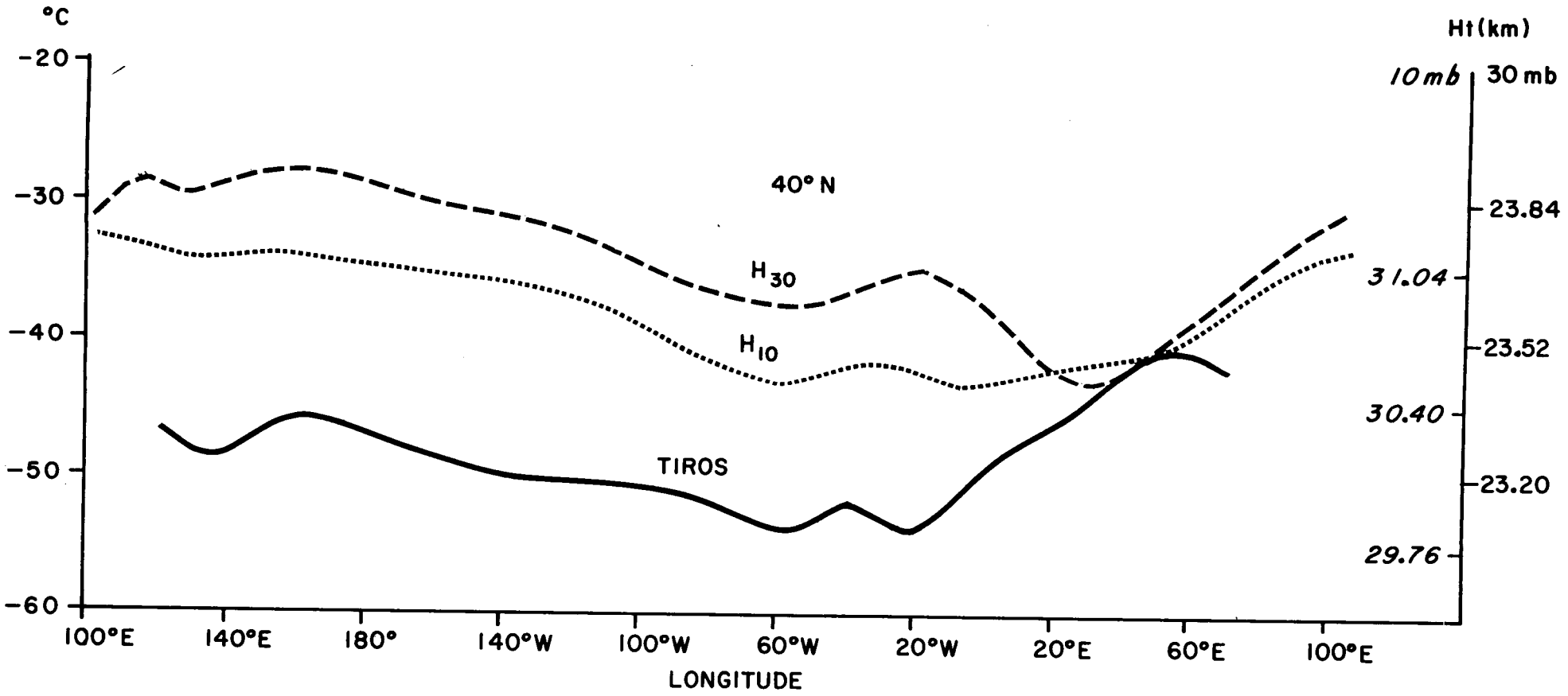

Figure 5c 30-mb and 10-mb heights and 15-micron temperature versus longitude at 40N, for 27 January 1964

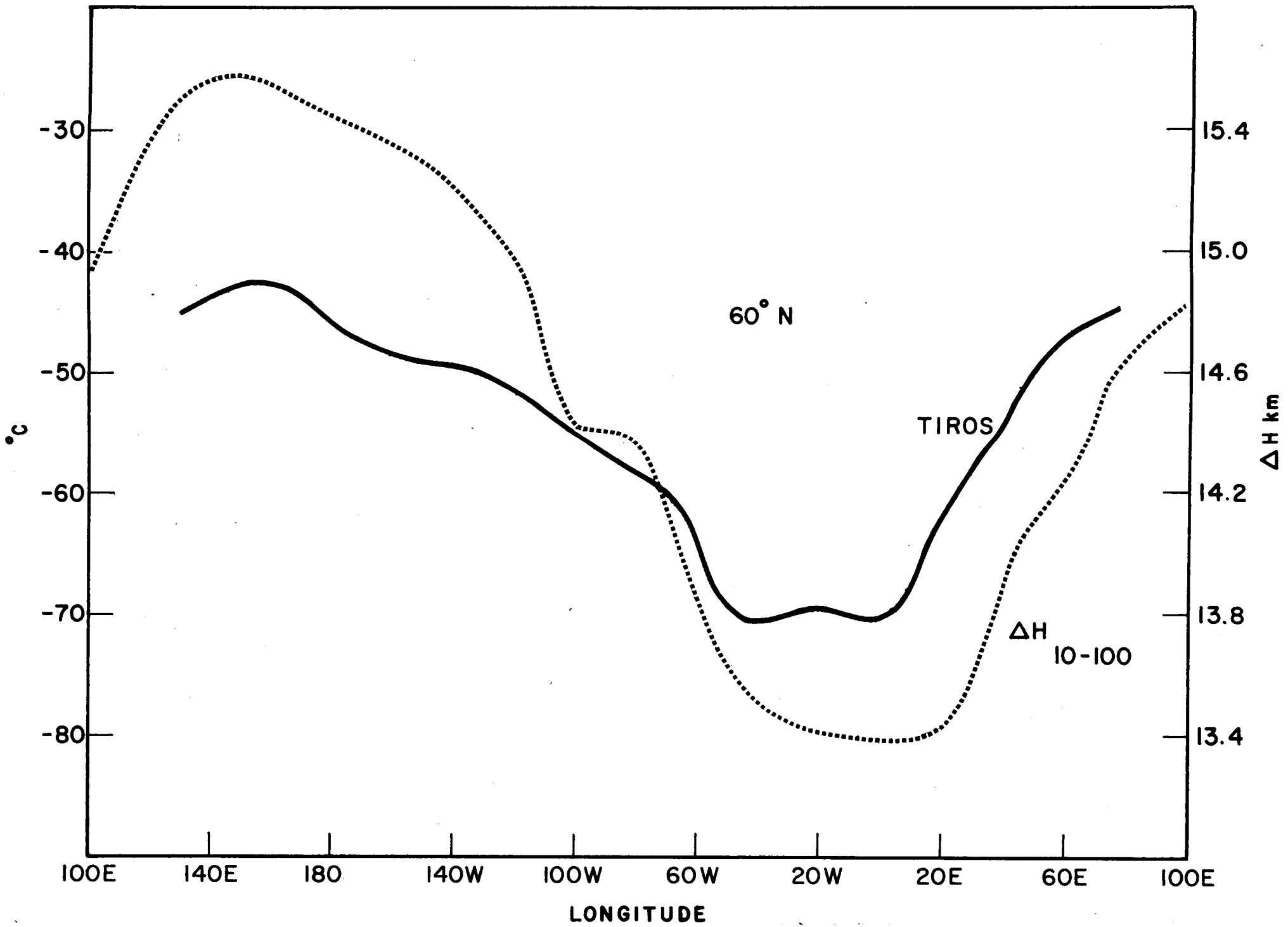

Figure 6a 10-mb to 100-mb thickness and 15-micron temperature versus longitude at 60N, for 27 January 1964

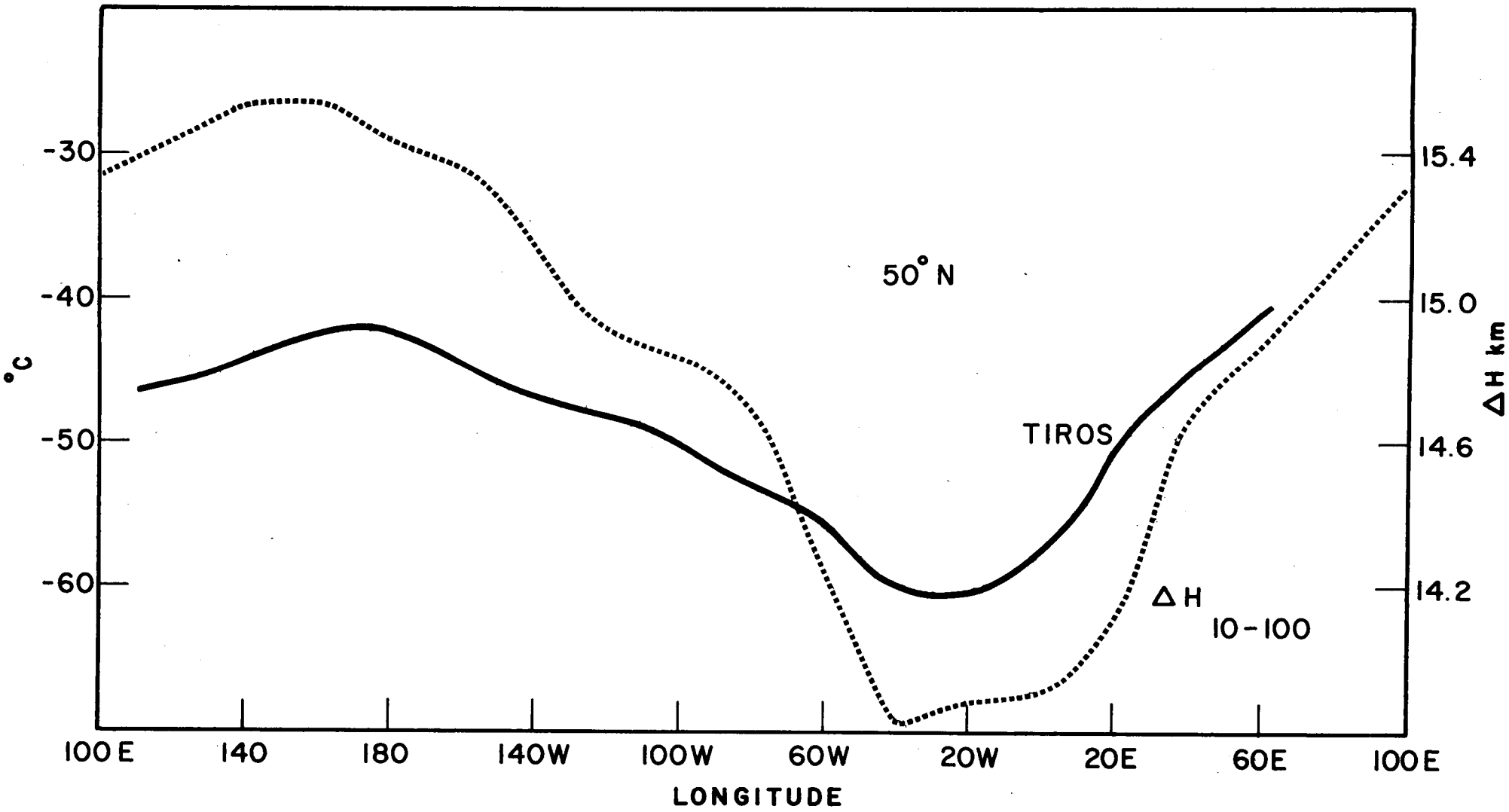

Figure 6b 10-mb to 100-mb thickness and 15-micron temperature versus longitude at 50N, for 27 January 1964

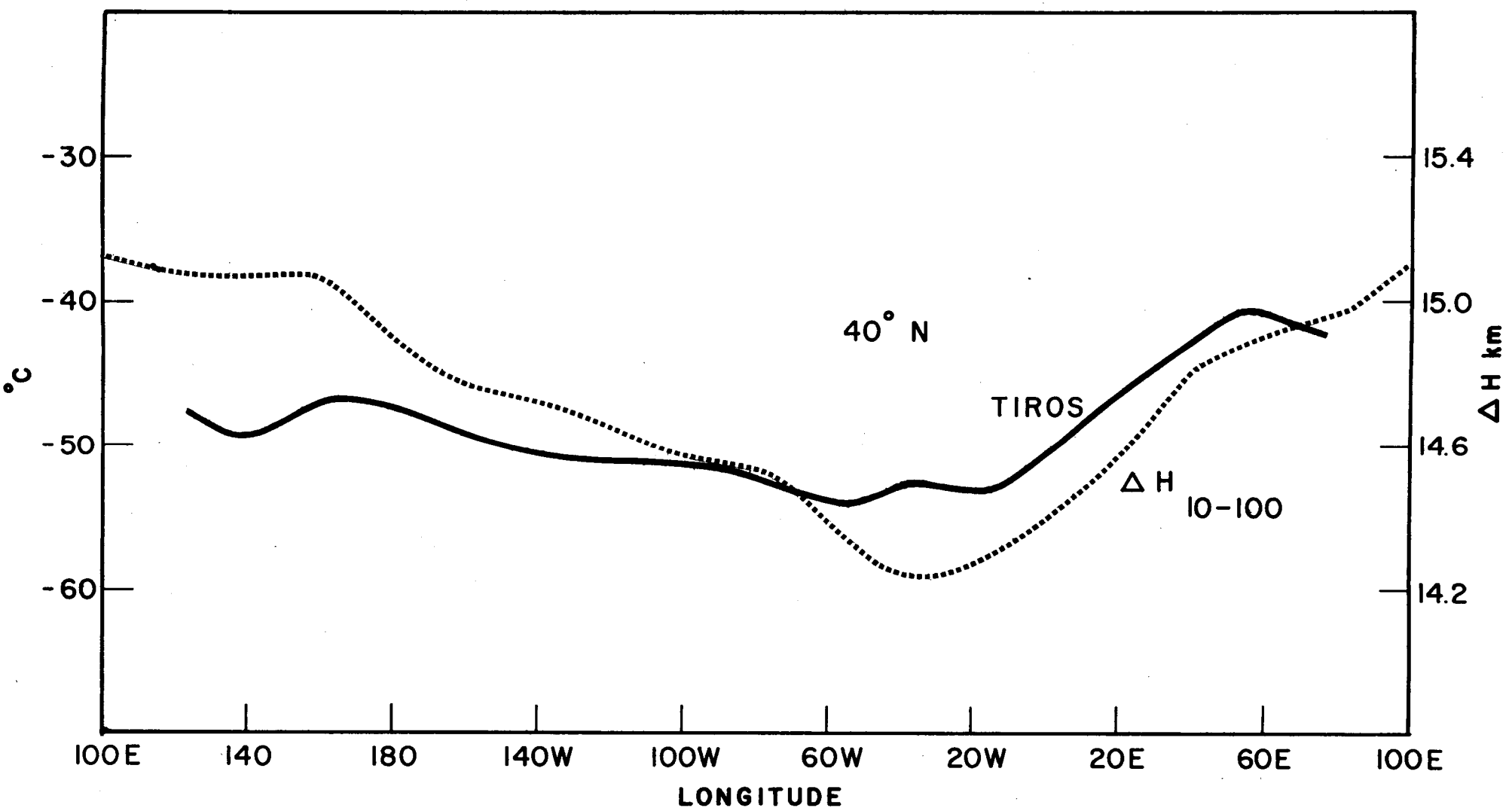

Figure 6c 10-mb to 100-mb thickness and 15-micron temperature versus longitude at 40N, for 27 January 1964

Research Division
CONTROL DATA CORPORATION
Minneapolis, Minnesota 55440

FINAL REPORT
Contract NAS5-10171

Paper II

ANTARCTIC STRATOSPHERIC WARMINGS DURING 1963

REVEALED BY TIROS VII, 15-MICRON DATA

Prepared by:

W. C. Shen
G. W. Nicholas
A. D. Belmont

for

NATIONAL AERONAUTICS AND SPACE ADMINISTRATION
Goddard Space Flight Center
Glenn Dale Road
Greenbelt, Maryland 20771

2 June 1967

ABSTRACT

TIROS VII 15-micron radiation data were used to study southern hemisphere stratospheric warmings during the winter of 1963, ~~over regions which had little conventional data.~~ Three significant warmings could be mapped despite the latitudinal limit of 60S. The first, from 20 July to 13 August, and the second from 26 August to 16 September each reached a maximum in the Australian sector, ~~with temperature~~ increases of 10C and 24C near Campbell ~~Island. The warmings~~ moved ~~eastward from Australia~~ and the South Indian ~~Ocean.~~ The third, or final warming, occurred in the Western South Pacific from 16 October to 10 November, ~~with a temperature increase of 21C.~~ This warming travelled southeastward toward the South Atlantic Ocean. ~~This study demonstrates the~~ validity and usefulness of single-day satellite ~~data.~~ It is ~~strongly~~ suggested that future observations of the same, ~~narrow~~ carbon dioxide band be carefully processed to filter out only the random time fluctuations in order that this system's potentially high resolution in time and space can be realized. This waveband can ~~indeed~~ provide mid-stratospheric temperature data over the major portion of the globe which now has no upper-air observational network ~~at all.~~ Only a ~~truly~~ polar orbit would further provide such data over the central polar regions where this atmospheric layer experiences dramatic changes and is of most interest.

TABLE OF CONTENTS

(Figures 1-18 follow text)

LIST OF FIGURES

LIST OF FIGURES
(cont'd)

I. Introduction

Following the discovery of stratospheric sudden warmings by Scherhag, (1952), numerous reports (for example, Finger and Teweles, 1964; Wilson and Godson, 1962) have appeared describing their behavior and characteristics in the northern hemisphere. Several warmings of various intensity usually occur each winter. In addition to these, in the springtime, there is a final warming which is associated with the seasonal reversal of meridional thermal gradient and the replacement of the cold polar vortex by a warm anticyclone. They affect not only the circulation but also the density distribution in the lower stratosphere. Similar events have been observed in the southern hemisphere (Godson, 1963). However, the sparseness of observations, particularly in the southern oceans, makes analysis and subsequent description of stratospheric events difficult.

The 1963 stratospheric warmings of the southern hemisphere were first pointed out by Nordberg et al (1965) using 15-micron data. They found that a warm region over the southeastern Indian Ocean persisted throughout the winter and then spread to make one half of the hemisphere almost 15°K warmer than the other. However, no details of the warming were given. Phillpot (1964) discussed the 1963 final warming in the Antarctic region using radiosonde data. Teweles (1966) compared the TIROS 15-micron temperatures with the radiosonde temperatures at two stations and indicated that there existed two stratospheric warmings. Briggs (1965) using rocketsonde data found the final warming in the spring but failed to detect the mid-winter warmings. Quiroz (1966) reanalyzed Brigg's data and demonstrated

that a major warming occurred in July-August, and concluded that the same warming was delayed until September at lower levels.

The problem of evaluating the southern hemisphere warmings can be improved by using more detailed satellite radiometric measurements from the 15-micron carbon dioxide emission band. The sensor characteristics and theoretical evaluation of the 15-micron temperatures[1] have been described by Nordberg, et al (1965) and Bandeen, et al (1965). These temperatures are vertically weighted mean temperatures; 65 per cent of the radiative energy in the band centered at 15-microns originates from 15 to 35 km. The maximum emission at low nadir angles is at 23-25 km. In a companion paper in this report, it is shown that the 15-micron temperatures can be interpreted as equivalent to the 20- or 30-mb temperatures. The near global coverage from 60N to 60S, of these stratospheric temperatures makes them an important source for studying southern hemispheric and oceanic events. The purpose of this paper is to investigate the features of the sudden warmings in the southern hemisphere winter and spring of 1963 revealed by the TIROS VII 15-micron temperatures.

[1]In this report the temperatures derived from the 15-micron channel radiative intensities will be referred to as 15-micron temperatures.

II. Data

Three different sets of 15-micron temperature maps were used. One set was the 10-day mean maps compiled by Kennedy (1966) which were spatially filtered and had isotherms drawn by a computer. Two spatial filters were used to retain the longest waves unchanged in amplitude and phase, but to eliminate short waves. The filters effectively eliminated waves shorter than about 20° in the zonal direction, and from 20° to 10° in the meridional direction from 0 to 60° latitude. The advantage of averaging over time and space was to smooth the random noise of the radiation signal and to extrapolate over gaps between orbital paths and regions not covered by the satellite. All observations that are located in a rectangular area are averaged and the average value applied to the center of the area. For the 1:40 million Mercator map used for this set of maps, the length of the rectangle is constant at 5° of longitude, but the width varies from about 5° of latitude at the equator to 2.5° of latitude at 60 degrees. A 10-day period consolidates 20 to 70 orbits and, as a result, each grid-point average generally contains several hundred observations. If the grid-point average contained less than 40 observations it was discarded from the automated isotherm analysis. A disadvantage of the 10-day maps is, of course, that temperature variations with periods less than 10 days are averaged out. To recover some of the lost information from the 10-day maps, single-day maps were examined.

The second set was a group of 50 usable individual day maps over a 127 day period from 15 July to 19 November. The maps were the normal Mercator

grid-print maps of 1 to 40 million scale described by Staff Members (1962) and the same as used in the first set of maps above. On these maps, isotherms were drawn by hand, to the grid-point average if it contained 10 or more observations. The data for these maps were not filtered.

The third set consisted of 7 single-day maps selected from the 127 day period of set two, to show the temperature minima and maxima before and during the three warmings, and they are reproduced in this paper. These maps were plotted and analyzed using the same computer program that produced the 10-day mean maps with two exceptions: grid-point averages from 10 or more observations were retained, and the isotherms were in increments of 5C instead of 2C.

All of the temperatures were corrected for instrumental degradation by methods given by Staff Members (1965). Although each map extends from approximately 60N to 60S there are certain silent areas and data coverage depended upon the number and location of orbits which were available for single days. The number of orbits per day varied from 4 to 8. For the remainder of this report, "15-micron temperatures" will be understood to be from the 10-day mean maps unless individual day maps are specifically referred to.

Radiosonde data, which covered the Australian sector plus four Antarctic stations, were obtained from the Environmental Science Services Administration. Only a few of the soundings extended beyond 70 mb and thus analysis of these temperatures was restricted to 70 mb. Additional data were extracted from published reports by Phillpot (1964), Briggs (1965) and Teweles (1966).

III. Southern hemisphere warmings

The 15-micron temperatures at 60S, 170E, taken from the 10-day mean maps were plotted as a function of time as shown in Fig. 1. The plotted point applies to the mid-day of the 10-day period. Since the data were smoothed by averaging and filtering they do not show the short quasi-periodic oscillations demonstrated by Teweles (1966). They retain only longer period waves. Fig. 1 also contains a time plot of 15-micron temperatures for the same geographic point taken from the single-day maps, as well as for 50S, 170E for every other day from 15 July to 12 November except for a period from 30 July to 15 August when complete data were not available. Both of these curves show short-period oscillations that are not found in the 10-day mean time plot. The 30-mb radiosonde temperatures for Campbell Island (53S, 169E) taken from Fig. 1 of Teweles (1966) paper are included to verify that the short-period temperature waves found in the single day maps are real and not a result of the random noise of the radiation signal. These single-day 15-micron values thus permit a more accurate determination of the warming period than the 10-day means.

Fig. 1 shows three major temperature waves from July to November 1963. The approximate dates of the warmings at 60S, 170E are:

First warming	20 July - 13 August
Second warming	26 August - 16 September
Third warming	16 October - 10 November

First (mid-winter) warming

As the southern hemisphere winter progressed, the stratospheric temperatures decreased, especially in the Antarctic region, due to the seasonal reduction of solar heating. A very strong cyclonic vortex developed near the South Pole.

From the middle of June to early August the 10-day mean maps show that the isotherms south of 40S were practically parallel to latitude circles with the coldest temperatures at high latitudes. Slight deviations from a zonal pattern occur in the isotherms in the eastern South Pacific and south Indian Oceans. These areas are somewhat cooler than adjacent areas. The Pacific cold trough is much more persistent than the one in the Indian Ocean. It will be seen later that the western side of the Pacific cold trough is the site for the stratospheric warmings in this year. Fig. 2 shows the typical stratospheric thermal pattern for the southern hemisphere winter on 15 July. By early August, it appears that a warm air pocket had developed and by 12-13 August a definite warm area was located over the Australia-New Zealand sector as shown in Fig. 3.

During this mid-winter warming of early August, the warm air region expanded eastward and apparently southward. It was centered at 40S, 170E on the 10-day mean isotherm map of 9-18 August. Meanwhile, the southern vortex shifted to the Weddel Sea and the warm pocket intensified reaching its peak values. Afterwards, the southern vortex retrogressed to the South Pacific and the warm center weakened. This warming reached its final stage by the 18-27 August map period.

The 15-micron temperature change determined from the 10-day mean maps during an 18 day period from 26 July to 13 August, is summarized in Fig. 4. The 15-micron temperature increased 10C near the center located near 45S, 170W. The warming is predominantly zonal along 45S. The periphery of the warming extended as far east as Argentina, and west to Marion Island. On the other hand, no significant temperature increase is seen equatorward of 30S.

Although this first warming was not as remarkable as the more intense warming observed with the 15-micron data in the northern hemisphere in January 1964 (Nordberg, 1965), the rate of warming, nevertheless, was appreciable. The 10-day mean 15-micron temperatures at 60S, 170E reached a minimum -64C on 26 July as shown in Fig. 1. The temperatures increased to -55C on 9 August, a mean warming of 9C. By 27 August they had returned to the original level of -64C, suggesting that the warming was dynamic in nature, associated with wave perturbation.

The single-day temperature curve in Fig. 1 shows an increase of 16C from 20 July to 13 August at the same location and a subsequent cooling of 20C by 26 August. According to Rocketsonde measurements at McMurdo Sound (78S, 168E), temperature data indicates that the warming was greatest at 30 km, perhaps 40C from mid-July to mid-August according to Quiroz (1966). This mid-winter warming was also observed by radiosonde at Macquarie (55S, 159E) and Wilkes (66S, 111E) illustrated in Fig. 5. The 70 mb temperatures at Macquarie show the warming occurring in two waves with an increase of 6C from 21 July to 4 August and a subsequent decrease of 9C in the next nine

days with another surge of warm air that increased the temperature 8C from 13 August to 18 August. The single-day 15-micron temperatures at 50S, 170E also show this warming to occur in two waves as the temperature increased by 12C from 28 July to 13 August; decreased by 6C to 17 August, then increased again by 5C to 22 August. There were no data available at Wilkes between 18 July and 2 August, but after this time, the temperature at 70 mb decreased by 9C to 8 August, afterwards an increase of 12C occurred by 23 August. At 50 mb (not shown) the temperature increased by 14C from 8-23 August. Although the 10-day mean 15-micron temperatures indicate that some increase of temperatures should have occurred at Hobart (43S, 147E), the radiosonde data does not show an increase during late July and early August. Unfortunately, there were insufficient single day 15-micron data at this time and place to help clarify the situation. A significant warming of 14C, however, occurred earlier, between 16-22 July, and may be the same one which appeared about 10 days later, some 20° eastward and downstream of Hobart. The only data in the interior of the Antarctic continent is for 70 mb at Amundsen-Scott (Fig. 5) which shows no warming.

Fig. 6 shows the trajectory of the warm air pockets for all three warmings of 10-day mean periods. The solid curve shows a reasonably reliable trajectory and the dashed curve an extrapolated trajectory. The first warming originated in the Australian region, and moved eastward from the end of July to mid-August. It disappeared by 18 August. By 9 August another warm pocket had formed almost half way around the globe near the southern Indian Ocean. This bipolar temperature wave affirms Godson's (1963) climatology that bipolarity over the southern oceans, but not over the Antarctic, may

accompany the final warming. This dual warm stratospheric wave was evident in the 10-day maps from this time to the end of the final warming at mid-latitudes. Only a single wave was evident, however, around the 60S latitude circle.

Second warming

The 15-micron temperatures at 60S, 170 E reached a minimum of -64C as shown by the 10-day mean map centered at 28 August. The middle stratosphere had warmed to -40C at this location by the map time centered at 16 September, a warming of 24C. The same maps show a warming of 15C and 9C at 50S, 170E and 40S, 170E, respectively. The single day map of 26 August shown in Fig. 7 indicates that the 15-micron temperatures at 60S, 170E had experienced a considerable decrease from 12-13 August reaching values less than -73C, much below what they were before the warming in July. This cooling is verified by the 30-mb temperatures at Campbell Island in Fig. 1. Fig. 8 shows that the middle stratosphere at this same location had warmed to about -38C by 15 September, a warming of 35C.

The 10-day mean maps reveal that a definite warm center had developed near 40S, 75E by 18 August. It moved southeast until 16 September when it was located near 52S, 150E; then it veered to the northeast and by 20 September the warm center was located near 35S, 165E; it then disappeared. Fig. 9 shows that the maximum 15-micron temperature change from the 10-day maps from 28 August to 20 September was +24C at 60S, 170E. Increases of 8C or more occurred as far north as 35S in the New Zealand area. Significant warmings, however, occurred almost entirely around the globe at 60S. It

should be made clear that this is not the final warming when the stratospheric circulation pattern changes to a summer pattern. The 15-micron temperature maps demonstrate that substantial cooling occurred over most of the southern hemisphere before the final warming reached a climax in mid-November. However, this second warming may be considered a preliminary surge of the final warming because its final temperature was warmer than its initial value.

From the limited number of radiosonde stations available, the 70 mb temperature change chart (Fig. 10) places the center of maximum warming, 26C, toward Macquarie Island (55S, 159E). This center is slightly to the southwest of the center indicated by the 15-micron temperatures. One would have expected Campbell Island (53S, 169E) to show the maximum warming to be consistent with the locations of the 15-micron temperature changes. This small inconsistency may be due to the different levels in the atmosphere represented by the two temperatures. It is possible that the maximum warming occurred further to the southeast at levels above 70 mb which would be represented better by the 15-micron temperatures. It may be too that the maximum warming of the 10-day average 15-micron temperatures would shift the center slightly from the single day observation at 70 mb. Considering these reasons, and in view of the radiosonde confirmation, the 15-micron mean temperatures still established the location of the maximum warming with excellent accuracy.

The 24C warming of the 15-micron temperatures and the 26C warming at 70 mb for Macquarie Island indicate that a much larger warming may have

occurred at higher levels. The change of +13C in the 70 mb temperature at Campbell Island is exceeded only slightly at the 15 mb level (Fig. 5), indicating that almost equal warming occurred through a deep layer to low levels. On the other hand, Wilkes, which is much farther from the indicated maximum warming center than Campbell Island and beyond the 15-micron temperature coverage, had a warming of 56C at 10 mb compared to only 5C at 70 mb. Wilkes and Campbell Island were the only two stations available that had enough data above 70 mb to permit discussion of the vertical structure of the warming. From this limited data, one might conjecture that the warming reached considerably lower altitudes at its northernmost excursion, but was confined to much higher altitudes at its southern extreme.

It is interesting to note that Quiroz, 1966, interpreted the McMurdo rocket data as showing a high-level warming from mid-July to mid-August, and a delay of this same warming until September at 20 km. He also says "It is interesting to conjecture that if the warming at 20 km were examined without benefit of the higher-altitude rocket data, it could easily be construed as the beginning of the final (springtime) warming". The interpretation that is made here of the 15-micron temperatures which depict the thermal events very near 25 km, is that the July-August (first) warming took place at lower latitudes than McMurdo, and that the mid-September (second) warming was in fact the beginning surge of the springtime warming.

Third warming

The third warming may be considered as the last phase of the final warming of the 1963 southern hemisphere winter. The second and third warmings

reported here are considered together as the final warming following the description of the spring warmings by Godson (1963). Maenhout and Van Mieghem (1964), on the other hand, state that the Antarctic final warmings start after the spring equinox; by their criterion, the third warming discussed here would be the final warming and the second would not be a part of it but a mid-winter warming. In the opinion of the authors, the second warming is one surge of two that constitutes the final warming because the cooling that occurred after the peak of the second warming did not produce temperatures as low as they were before the onset of the second warming. At 60S, 170E, the 15-micron temperatures from the 10-day map decreased from -40C to -50C from 16 September to 14 October before the onset of the third warming. After 14 October these temperatures increased by 19C reaching a maximum of -31C on 15 November.

The single-day 15-micron temperature map for 1 October is presented in Fig. 11. The thermal pattern shows that warm air had spread into the South Atlantic and western Indian Oceans by 1 October, and the warm air over the western South Pacific had been replaced with relatively cool air. There is no zonal symmetry in the isotherms now and little south-to-north temperature gradient. Nevertheless, it appears that the spring reversal has not occurred as there is some general cooling around the globe at the higher southern latitudes until 14-15 October (Fig. 12). At 60S, 170E and 50S, 170E the temperatures decreased by 16C and 15C, respectively, from the 1 October single day map. The map for 19 November is given in Fig. 13, which shows that the spring reversal is complete and the isotherms have become organized

in a symmetrical pattern along latitude circles except over the area west of the Aleutian chain which, as usual, remains warmer than elsewhere at its latitude. The temperature at high southern latitudes increased to values of -23C to -33C. The stratosphere cooled by about 5C after this time, and then maintained its normal summer pattern indicating that the final warming of the winter had occurred.

The third warming followed the path shown in Fig. 6. Again, the solid curve indicates the track established by the 15-micron temperatures, and the dashed curve is its estimated continuation determined by extrapolating the 15-micron temperature pattern southward of its field of view, and supplemented the available radiosonde stations on the Antarctic continent. A warm center appears to have developed near 55S, 70E by 25 September. It moved eastward, then northeastward, until by 28 October it was located 60S, 100E, the southern limit of satellite coverage. Indications are that the center continued to move to the southeast as it was near 75S, 130W on 30 November, the latest date that the warm center could be located from available data.

Fig. 14 gives the 15-micron temperature change from the 10-day mean map centered at 14 October to the one centered at 21 November. Between these dates, a maximum warming of 21C occurred at 60S, 170W. Substantial warming had taken place almost around the southern hemisphere by this time, except in the eastern South Atlantic and southeastern Indian Oceans. The 10-day mean maps show that the latter area, which was warmer initially than

the Australian sector, did not reach its maximum temperature until the map centered at 5 December when a -27C isotherm ran along the 60S latitude circle between about 30E and 60W.

The 70 mb temperature change chart between 15 October and 20 November (Fig. 15) is strikingly similar to the 15-micron temperature change chart. At 70 mb the maximum warming extended along the 180th meridian from the pole to 65 or 70S. The location of the warming north of 60S is in good agreement with the location established by the 15-micron temperatures. From the stations along the Antarctic coast, it is quite obvious that the eastern South Atlantic and southwestern Indian Oceans had not obtained their maximum temperature by this time and subsequent warming occurred which is in agreement with the 15-micron temperatures. In a review of Antarctic final warmings, Godson (1963) states "it is general observation that temperatures tend to be warmer and final warmings to be earlier in the Australian sector than in South Atlantic sector". Maenhout and Van Mieghem (1964) also conclude that Antarctic stratospheric final warmings propagate across the South Pole from the Antarctic coast opposite Australia up to the Antarctic coast opposite South America. The year 1963 appears to be no exception.

IV. Comparison of the two hemispheric vortices

During the winter months, the stratospheric polar circulation is dominated by an intense cyclonic vortex centered close to the pole. The formation of the cold cyclonic vortex is the direct result of reduction and withdrawal of solar radiation. The circulation is predominately westerly. The antarctic and arctic vortices are similar in nature but not in detail. Satellite 15-micron temperature measurements make it possible to follow the variation of mean temperatures in the mid- and lower stratosphere from winter to summer at high latitudes (60°) from which inferences can be made about the polar circulation.

The distribution of the satellite temperatures in an antarctic vortex is shown in Fig. 16, which was derived from the 10-day mean temperatures established by Kennedy (1966). A large temperature gradient is seen from 45S southward toward the pole. The true polar-night circulation takes place south of 45S. Another feature of interest is a warm belt between 15-45S. Two warm centers are present in this warm belt during August 9-18, 1963, one near New Zealand and another in the south Atlantic and Indian Oceans. The warm belt shifts with season and the warm air pockets move predominately to the east.

To compare the stratospheric polar vortices in the northern and southern hemispheres, two periods, January-June 1964 and July-December 1963, were examined. The 10-day mean satellite temperatures along 60N and 60S from winter to summer were plotted respectively in Figs. 17 and 18. There were several interesting differences between antarctic and arctic winter circulations:

(1) In early winter the antarctic vortex is symmetrical while the arctic vortex is predominately asymmetrical to the pole. The variation of temperature along a latitude is insignificantly small in the southern hemisphere and large in the northern hemisphere along 60 degrees. The latter is as large as the temperature difference between summer and winter at 60N, 180° longitude.

(2) In mid- and late winter, warm centers occur near New Zealand and in the southern Indian Ocean. The southern polar vortex shifts toward the Weddel Sea. The asymmetry of the southern polar vortex is evident from increasing longitudinal temperature difference (10-12C at 60S). However, the degree of asymmetry of the antarctic vortex is always weaker than that of the arctic vortex. The asymmetry of the antarctic vortex of 1966 was also observed by the Nimbus II satellite (Nordberg et al, 1966). Furthermore, no bipolar pattern of the antarctic vortex was observed along 60S during the whole period.

(3) The antarctic vortex was more persistent throughout the winter than the arctic one. In 1963, the breakdown of the southern vortex took place 9 weeks after the spring equinox (i.e. the end of November). On the other hand, the breakdown of the arctic vortex occurred only one week after the spring equinox. The difference in timing may be due to stronger baroclinicity of the arctic vortex and the greater annual variability of final warmings in the northern hemisphere.

(4) The distribution of the summer stratospheric temperatures along 60S is uniform. This pattern is similar to the temperature pattern along 60N

latitude. However, in the southern summer, cooling of about 8C occurred after the peak of the final warming in late November, whereas in the northern summer no cooling is observed after the spring warming in this year and the high temperatures persisted through June. Data from Engberg and Belmont (1964) demonstrate that in some years such temperature drops are observed there also.

V. Conclusions and recommendations

Rocketsonde, radiosonde and 15-micron temperature data show that during the 1963 winter the antarctic area experienced two mid-winter warmings in addition to the final one. Although the preliminary satellite values in uncorrected form have already been used to show one apparent warming in the antarctic, this is the first application of the corrected TIROS VII 15-micron data to investigate the nature of the three warmings in some detail. This study also demonstrates the validity and usefulness of single-day satellite data. It is strongly suggested that future observations of the same, narrow carbon dioxide band be carefully processed to filter out only the random time fluctuations with frequencies less than a few seconds and not to filter data spatially, in order that this system's potentially high resolution in time and space can be realized. This waveband can indeed provide mid-stratospheric temperature data over the major portion of the globe which now has no upper-air observational network at all. Only a truly polar orbit would further provide such data over the central polar regions where this atmospheric layer experiences dramatic changes and is of most interest.

VI. References

Bandeen, W. R., M. Halev and I. Strange, 1965: A radiation climatology in the visible and infrared from the TIROS meteorological satellites. NASA TN D-2534, 1-30.

Briggs, R. S., 1965: Meteorological rocket data, McMurdo Station, Antarctic, 1962-1963. J. Appl. Meteor., 4, 238-245.

Engberg, L. W. and A. D. Belmont, 1964: Arctic stratospheric temperatures and densities. Final Report, Contract AF19-628-383, AFCRL, 64-806, 237 pp. Litton Systems, Inc., Minneapolis, Report LSI-2602 (AD610603).

Finger, F. G., and S. Teweles, 1964: The mid-winter 1963 stratospheric warming and circulation change. J. Appl. Meteor., 3, 1-15.

Godson, W. L., 1963: A comparison of middle-stratospheric behaviour in the arctic and antarctic, with special reference to final warmings. Meteor. Abhandl., Freien Univ. Berlin, Band XXXVI, 161-206.

Kennedy, J. S., 1966: An Atlas of Stratospheric Mean Isotherms Derived from TIROS VII Observations. GSFC document X-622-66-307, 85 pp. (Available from NASA, Goddard Space Flight Center, Greenbelt, Md.)

Maenhout, A. G. and J. Van Mieghem, 1964: Aanhoudende stratosferische verwarming in de lente boven de Koning Boudewijn Basis. Mededelingen van de Koninklijke Vlaamse Academie voor Wetenschappen, Letteren en Schone Kunsten van Belgie, Klasse der Wetenschappen, Jaargang XXVI Nr 10, pp. 30.

References (cont'd)

Nordberg, W., W. R. Bandeen, G. Warnecke, and V. Kunde, 1965: Stratospheric temperature patterns based on radiometric measurements from the TIROS VII satellite. Space Research V, Proceedings of the Fifth International Space Science Symposium, Florence, May 8-20, 1964, Amsterdam, North-Holland Publishing Company, 783-809.

Nordberg, W., A. W. McCulloch, L. L. Foshee, and W. R. Bandeen, 1966: Preliminary results from Nimbus II. Bull. Amer. Meteor. Soc., 47, 857-872.

Phillpot, H. R., 1964: The springtime accelerated warming phenomenon in the Antarctic stratosphere. International Antarctic Analysis Centre, Tech. Rep. 3, Melbourne, Commonwealth Bureau of Meteorology.

Quiroz, R. S., 1966: Mid-winter stratospheric warming in the Antarctic revealed by rocket data. J. Appl. Meteor. 5, 126-128.

Scherhag, R. A., 1952: Die explosionsartigen stratosphärenerwärwungen des Spätwinters 1951/1952. Ber. deut. Wetterd. (U.S. Zone), 38, 51-63.

Staff Members, 1965: TIROS VII Radiation Data Catalog and Users' Manual, 3, Greenbelt, Maryland, National Space Science Data Center, Goddard Space Flight Center, Code 601, 269 pp.

Staff Members, 1962: TIROS III Radiation Data Catalog, Greenbelt, Maryland, National Space Science Data Center, Goddard Space Flight Center, Code 601, 388 pp.

References (cont'd)

Teweles, S., 1966: Radiometer data in the 15μ band. In "Satellite Data in Meteorological Research", NCAR-TN-11, Boulder, Colorado, NCAR, 251-257.

Wilson, C. V., and W. L. Godson, 1962: The stratospheric temperature field at high latitudes. Arctic Meteor. Res. Gp., Publ. in Meteor., 46, Montreal, McGill University, 191 pp.

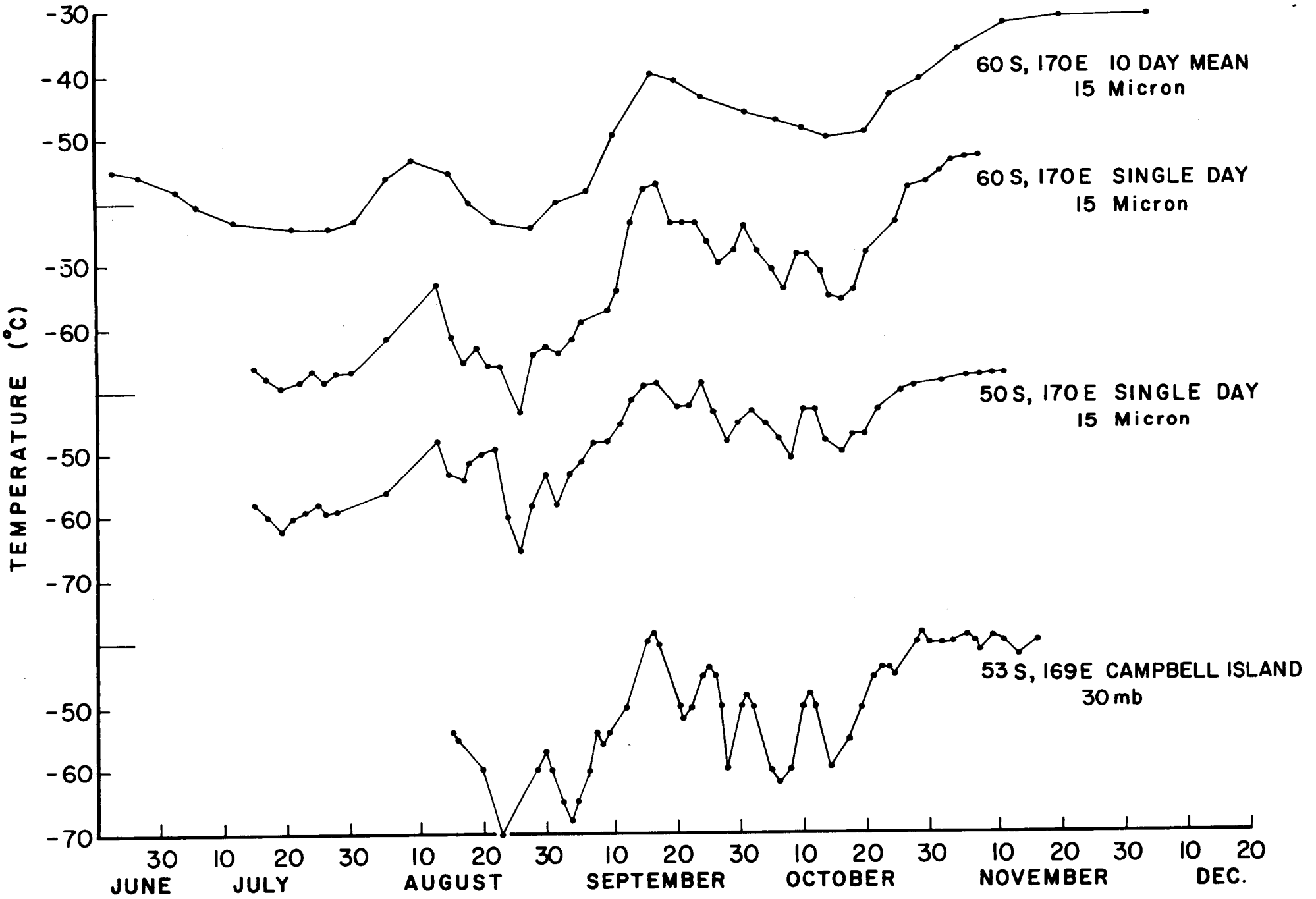

Figure 1 The 15-micron and 30 mb temperatures at Campbell Island

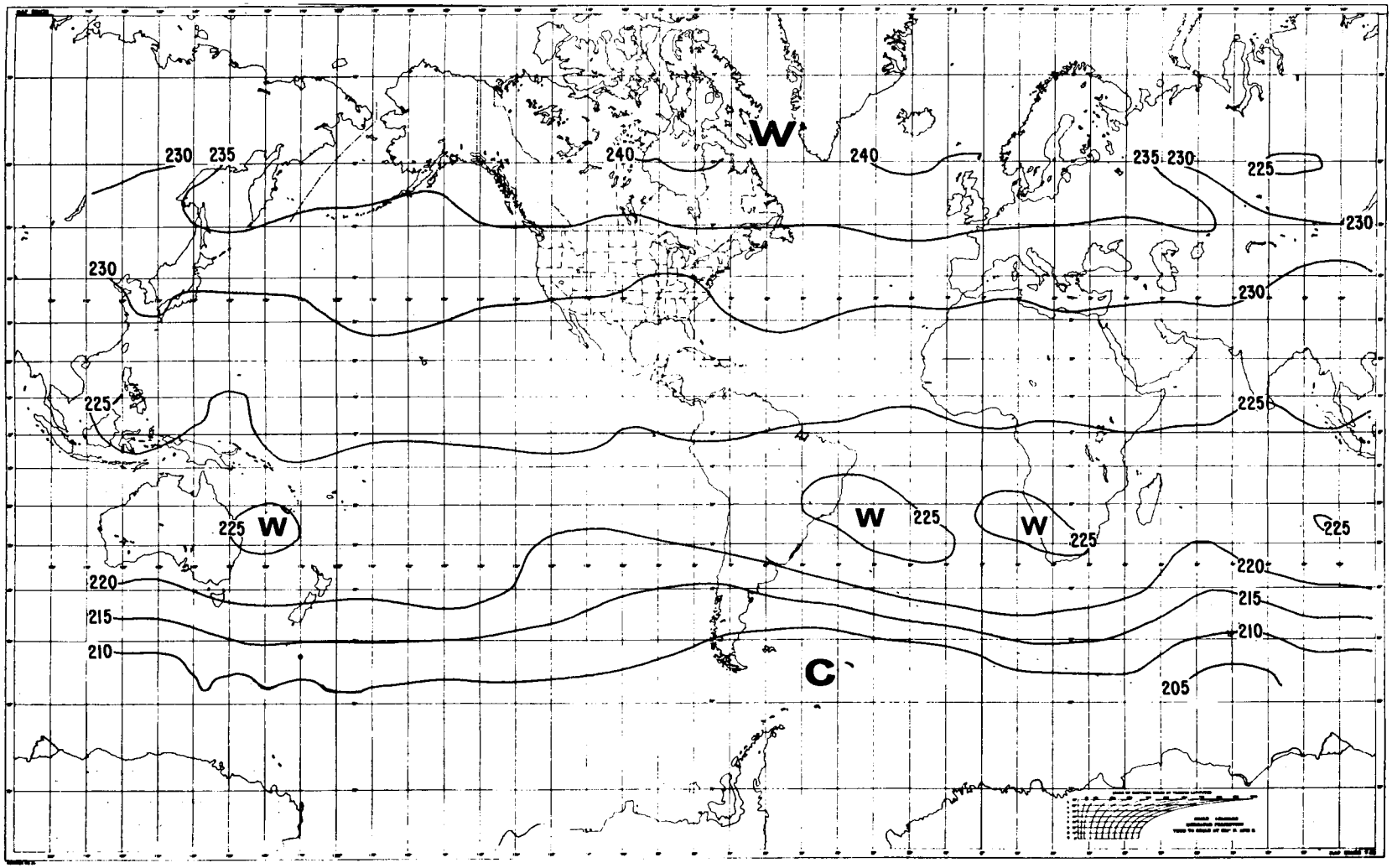

Figure 2 TIROS VII, 15-micron temperatures (°K) from 2330 GMT on 14 July to 1442 GMT on 15 July 1963

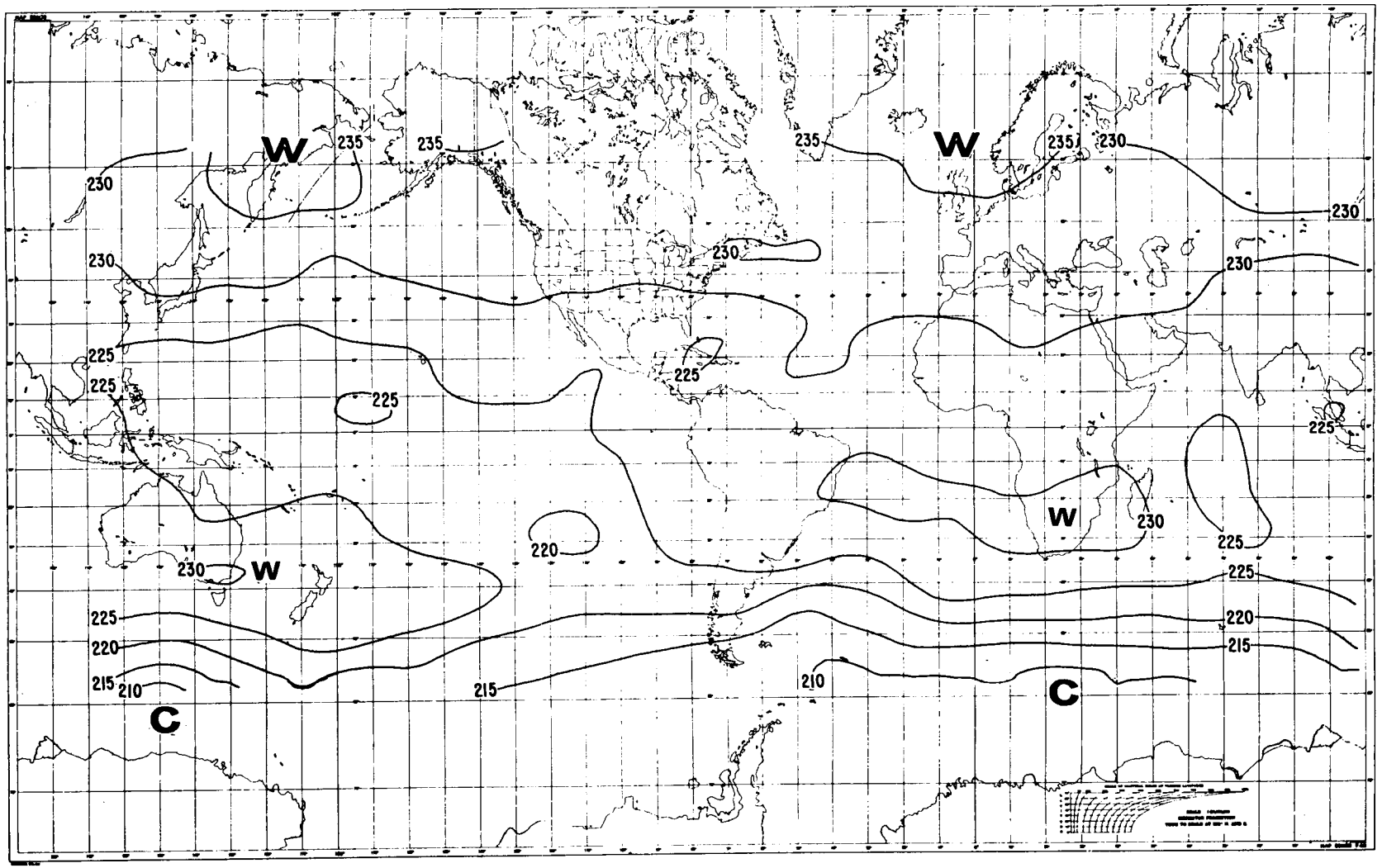

Figure 3 TIROS VII, 15-micron temperatures (°K) from 1423 GMT on 12 August to 0526 GMT on 13 August 1963

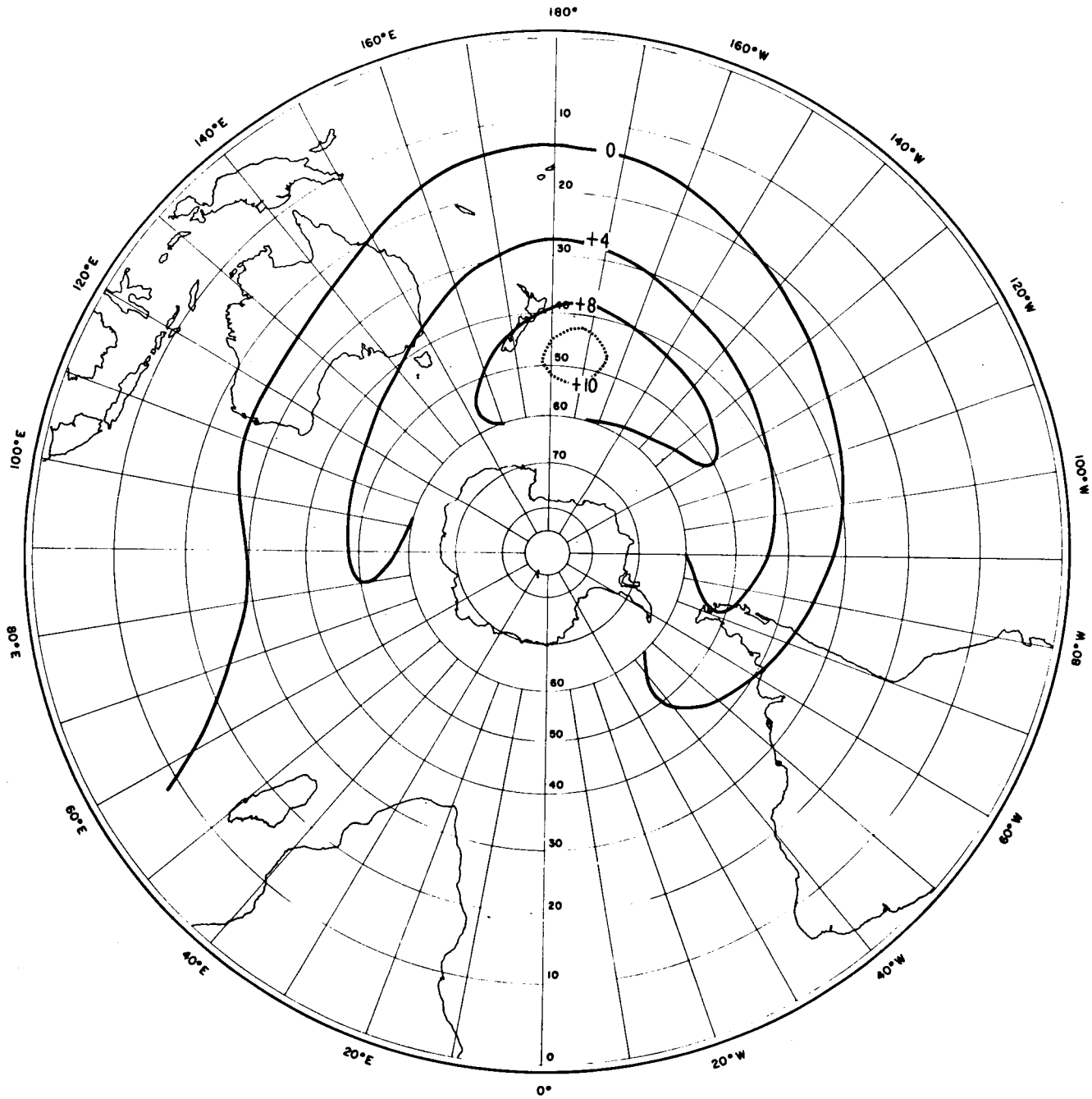

Figure 4 The 15-micron temperature change from 26 July to 13 August 1963 in the southern hemisphere taken from 10-day mean maps

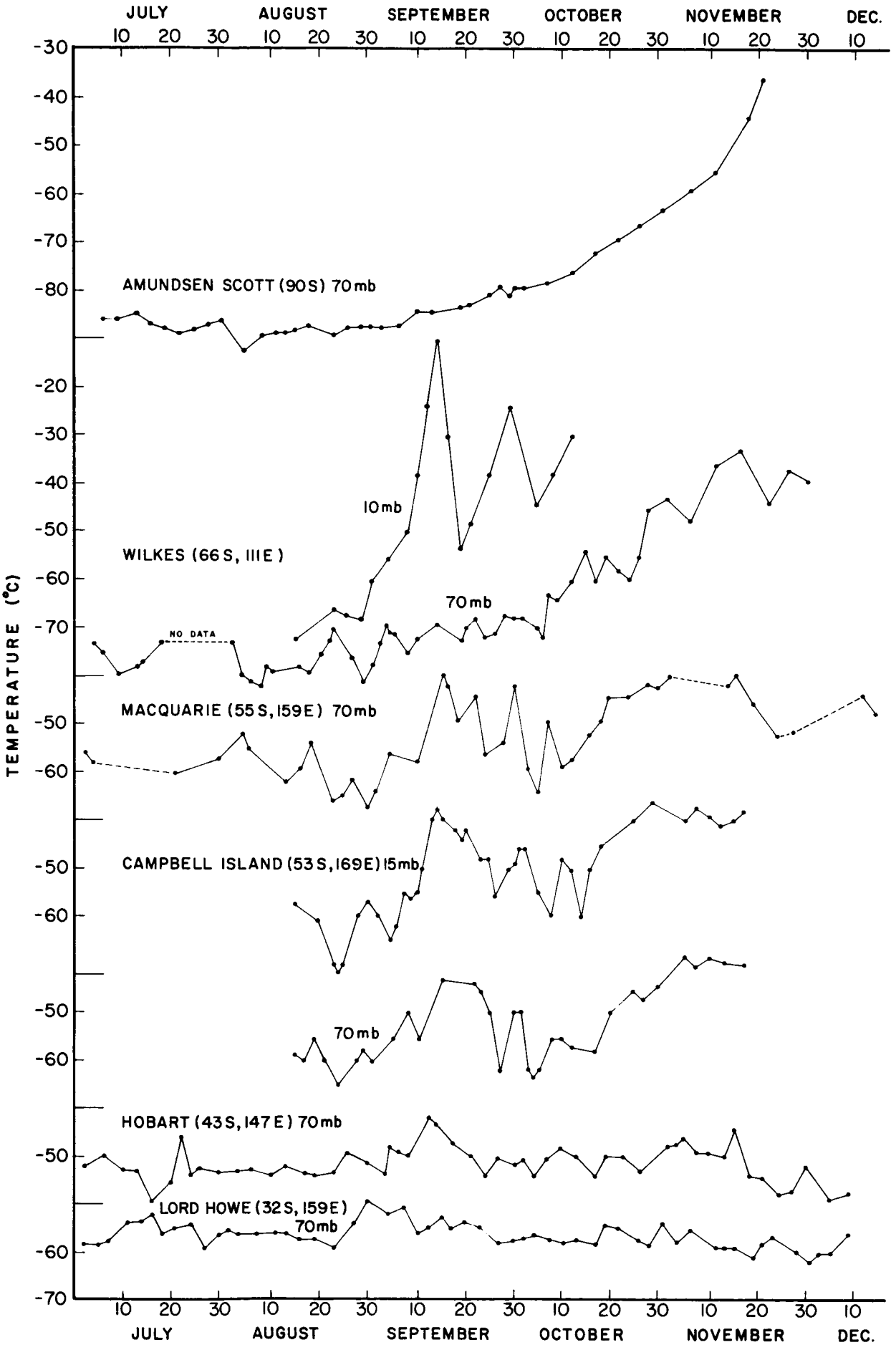

Figure 5 Radiosonde temperatures during the southern hemisphere winter of 1963 for selected available stations and pressure levels.

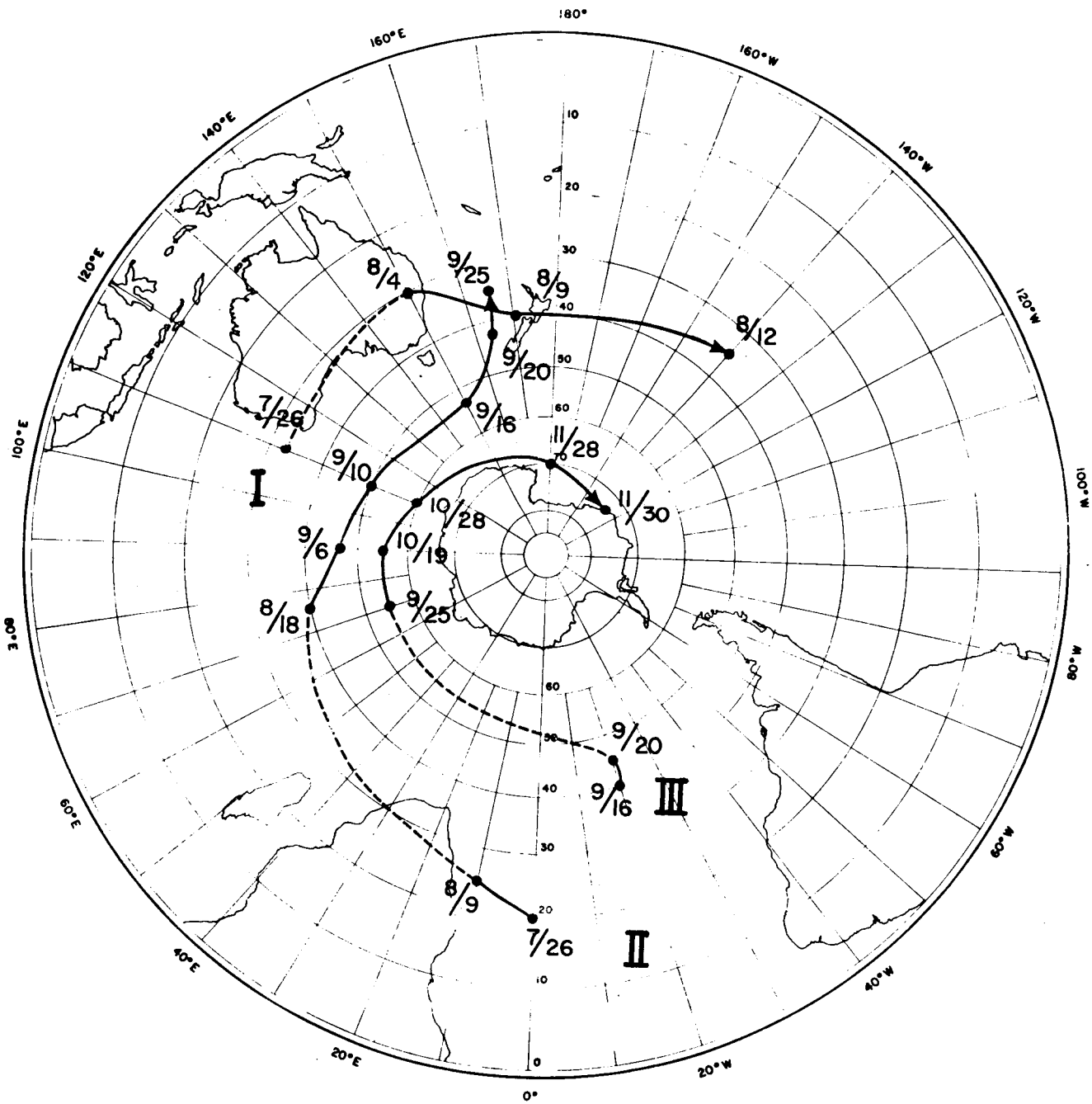

Figure 6 The trajectories of three distinct stratospheric warmings during the 1963 winter

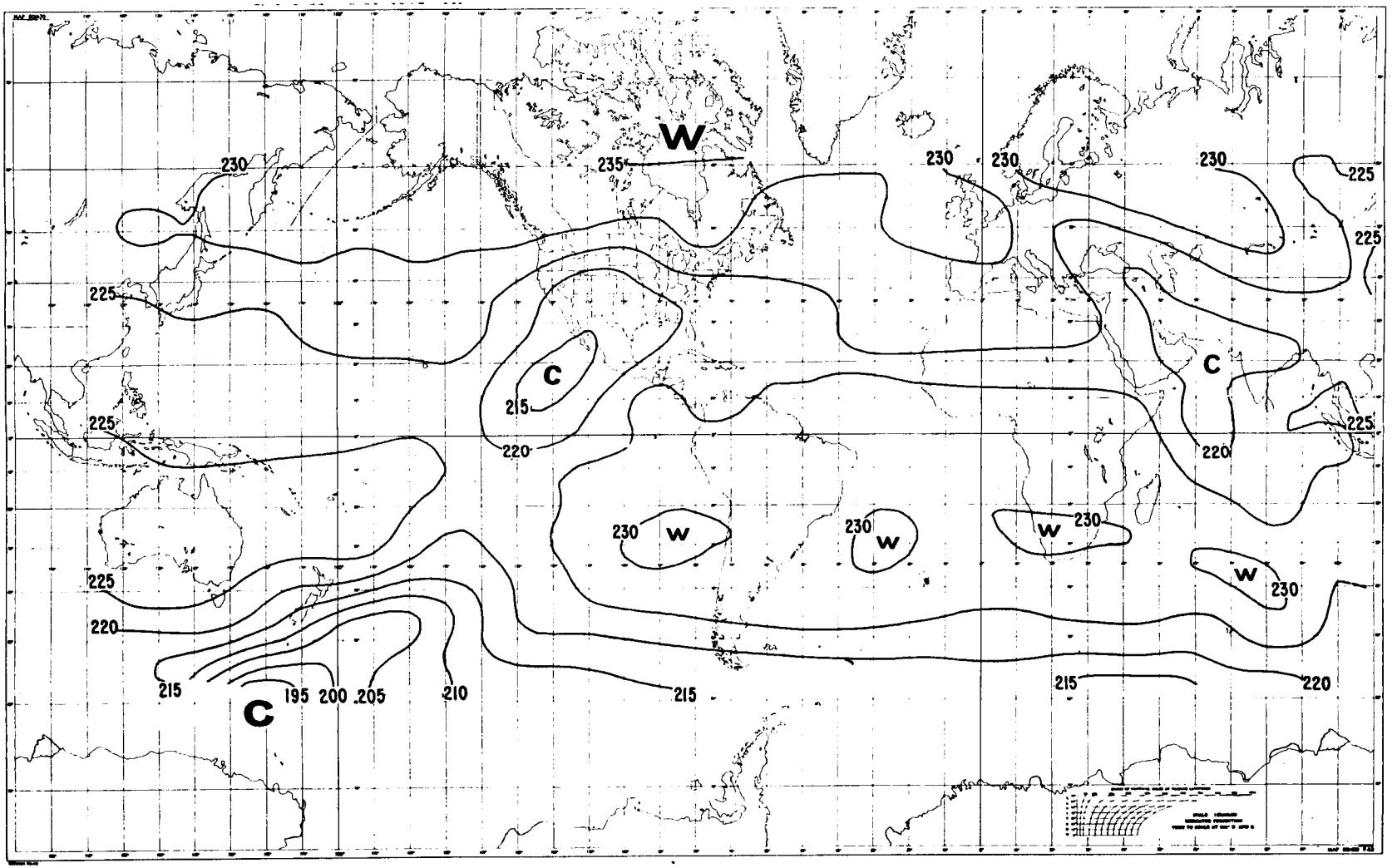

Figure 7 TIROS VII, 15-micron temperatures (°K) from 0932 GMT on 26 August to 0036 GMT on 27 August 1963

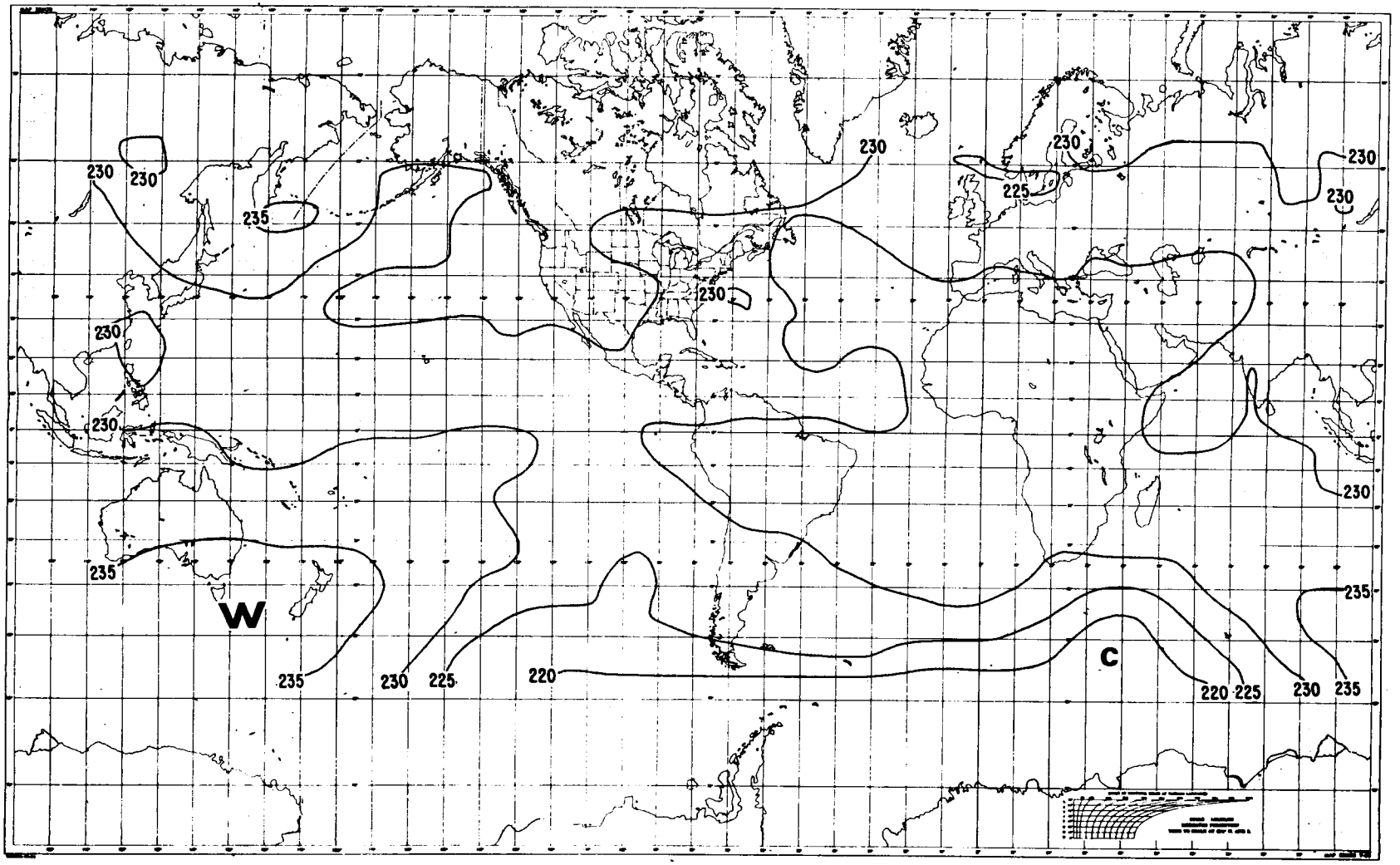

Figure 8 TIROS VII, 15-micron temperatures (°K) from 0345 GMT to 1841 GMT on 15 September 1963

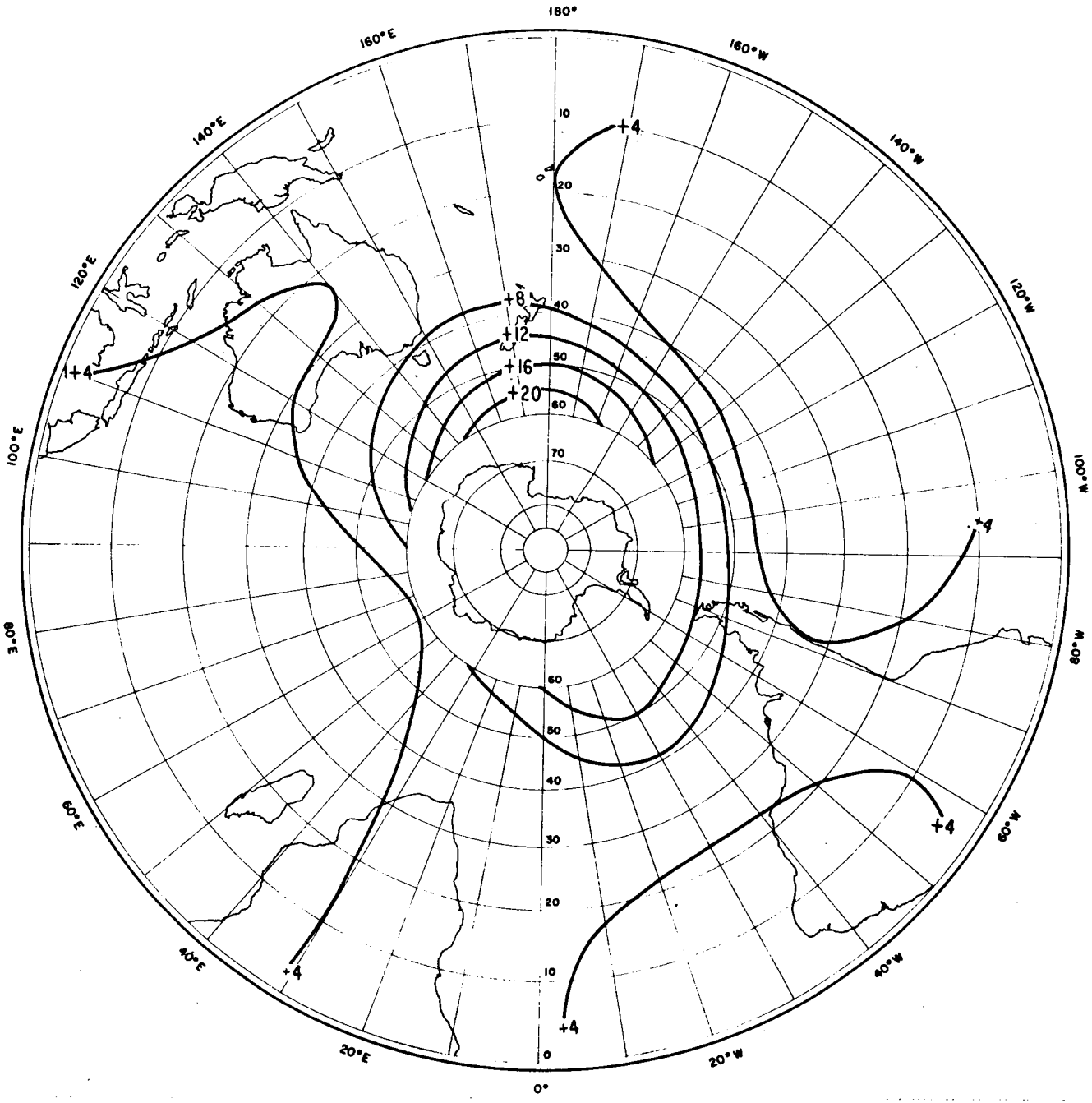

Figure 9 The 15-micron temperature change from 28 August to 20 September 1963 in the southern hemisphere taken from 10-day mean maps

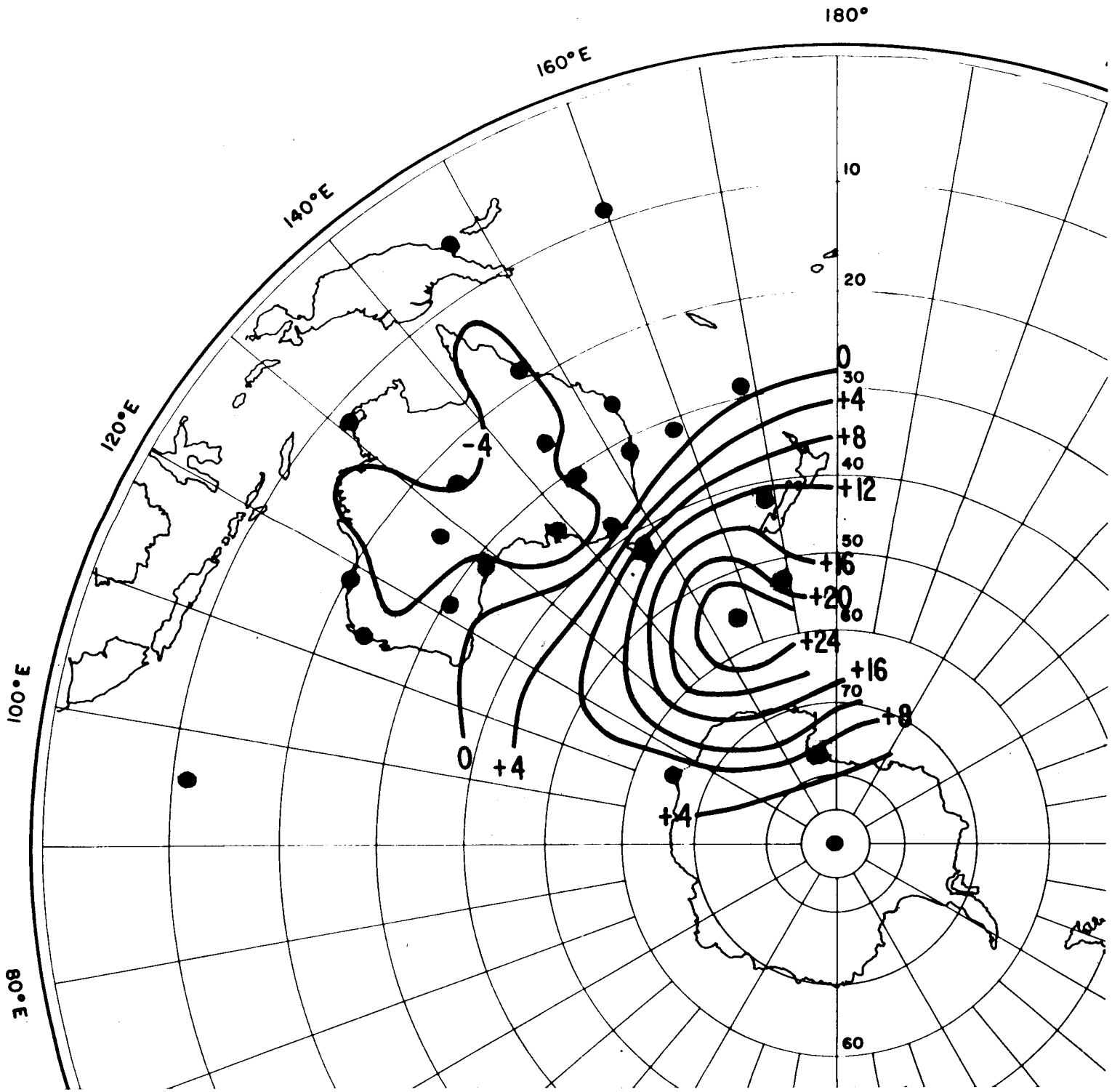

Figure 10 The 70 mb temperature change from 30 August to 16 September 1963 for available stations in the southern hemisphere

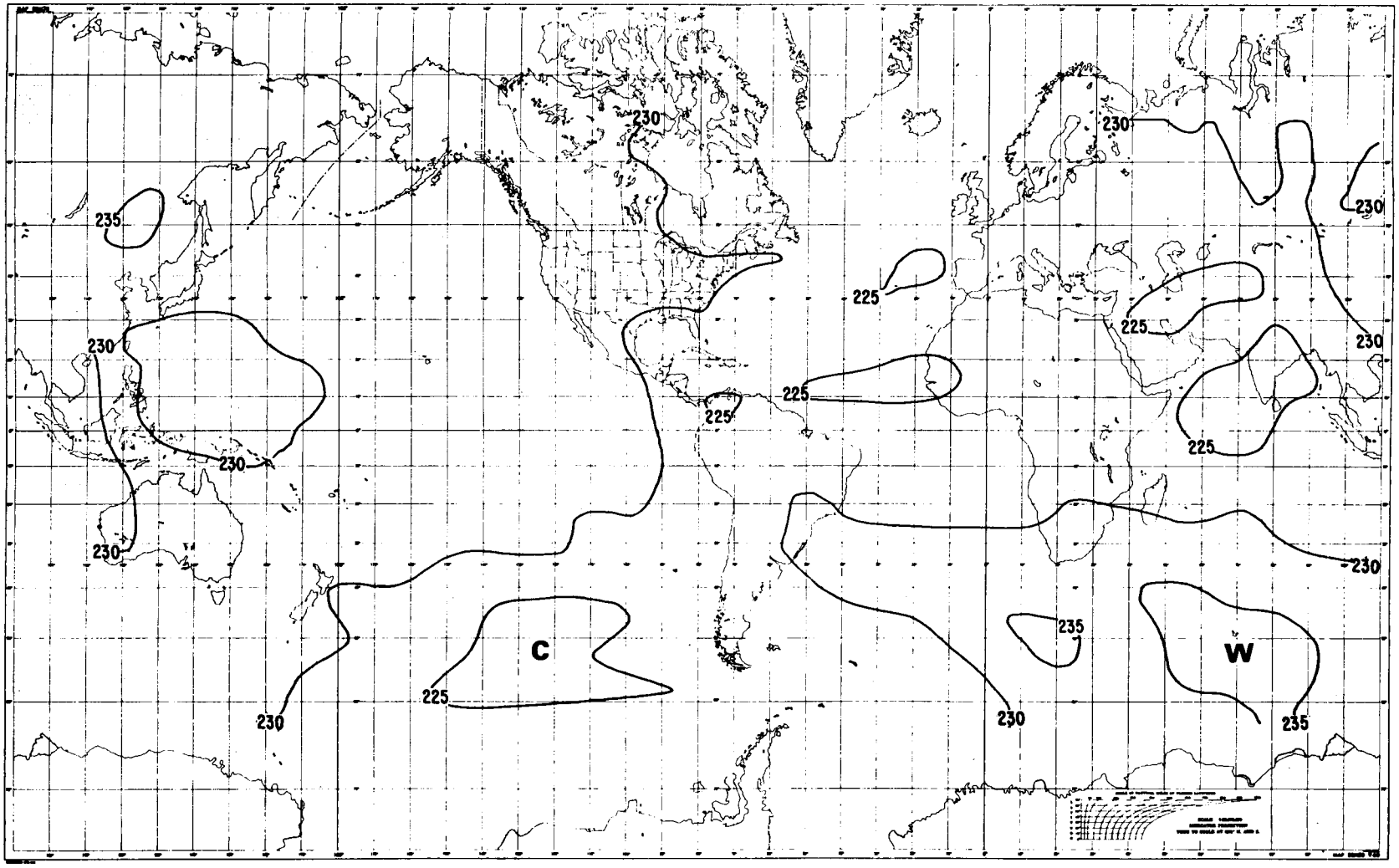

Figure 11 TIROS VII, 15-micron temperatures (°K) from 2334 GMT on 30 September to 1255 GMT on 1 October 1963

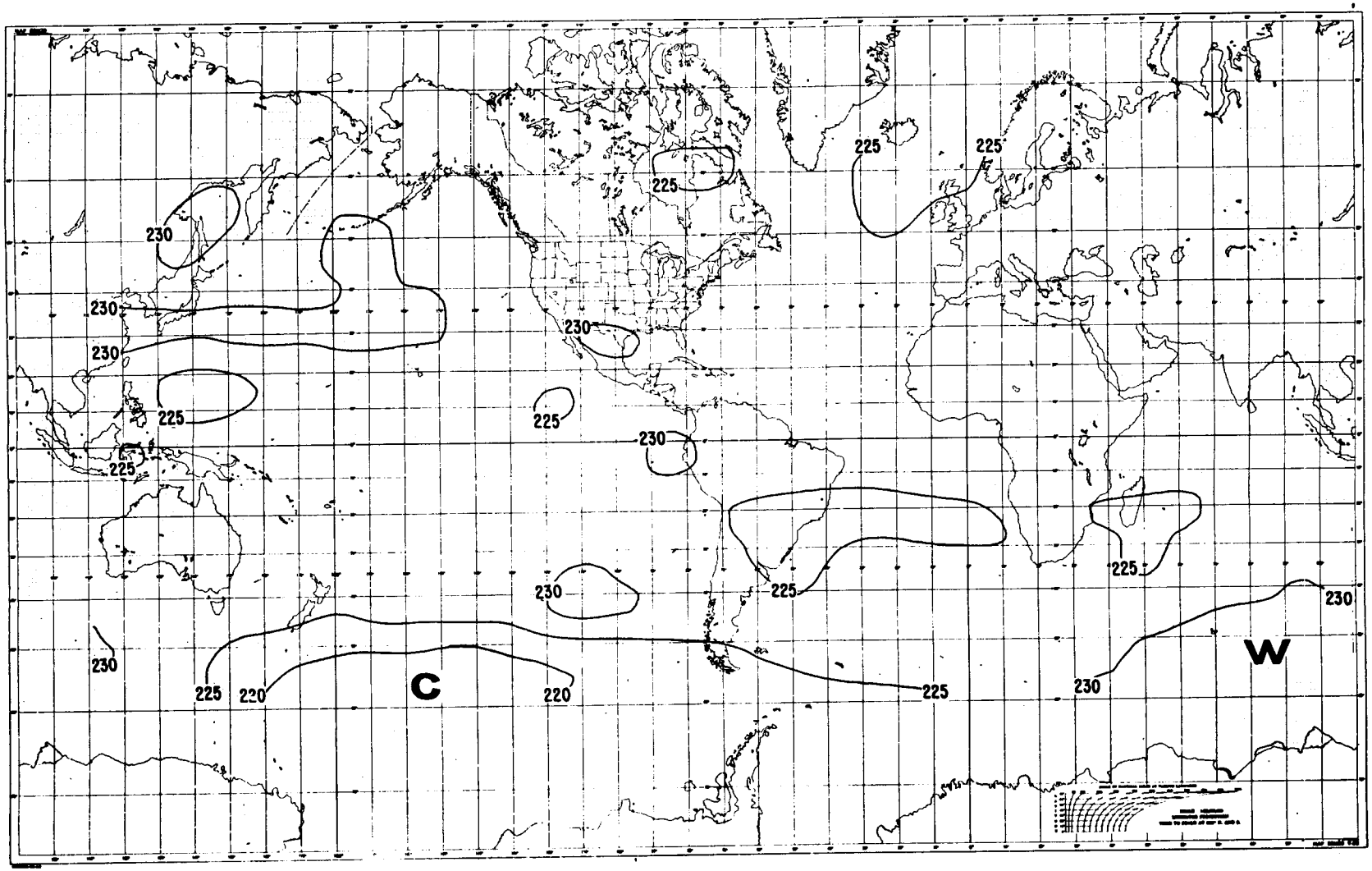

Figure 12 TIROS VII, 15-micron temperatures (°K) from 1844 GMT on 14 October to 0617 GMT on 15 October 1963

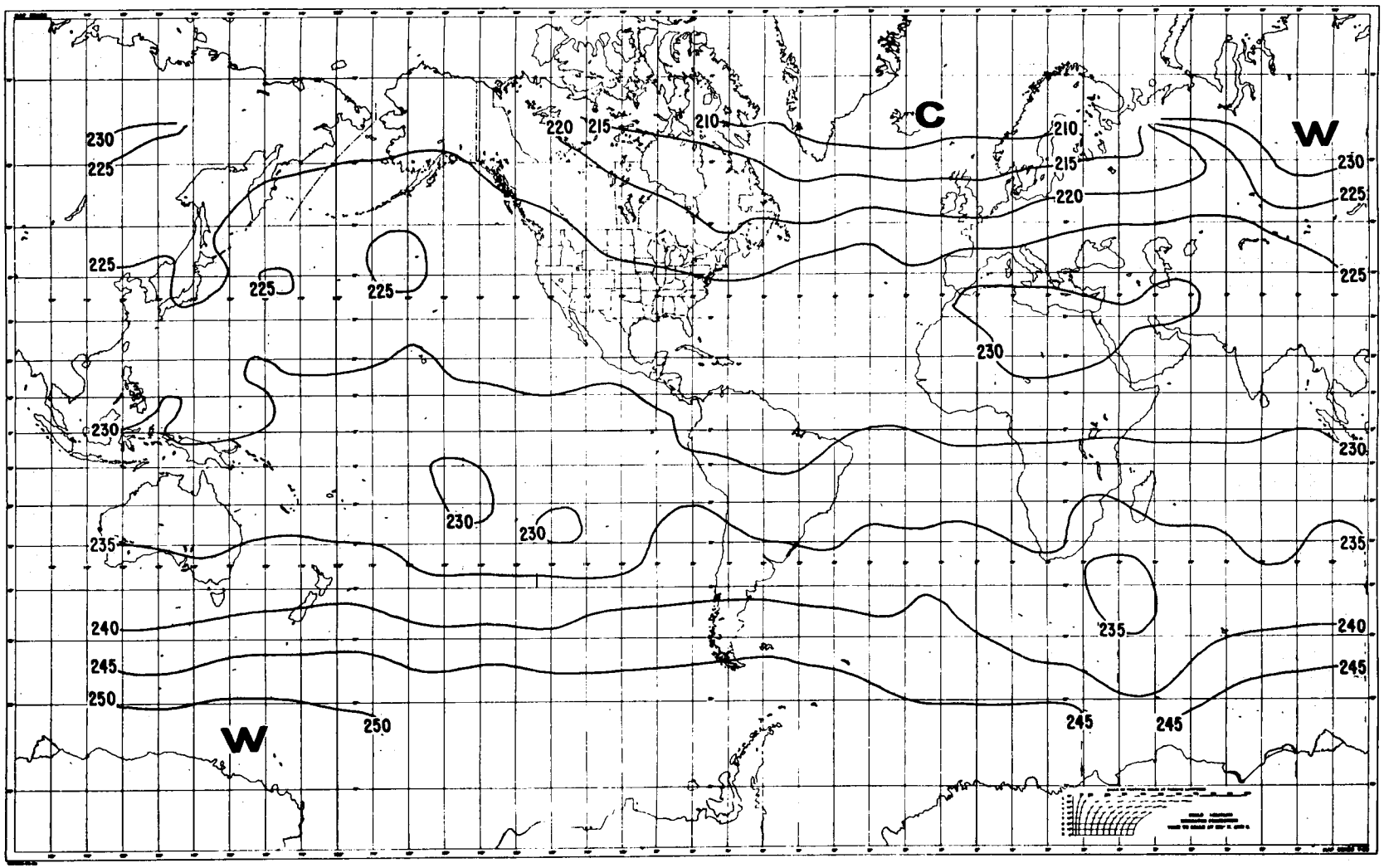

Figure 13 TIROS VII, 15-micron temperatures (°K) from 0652 GMT to 2206 GMT on 19 November 1963

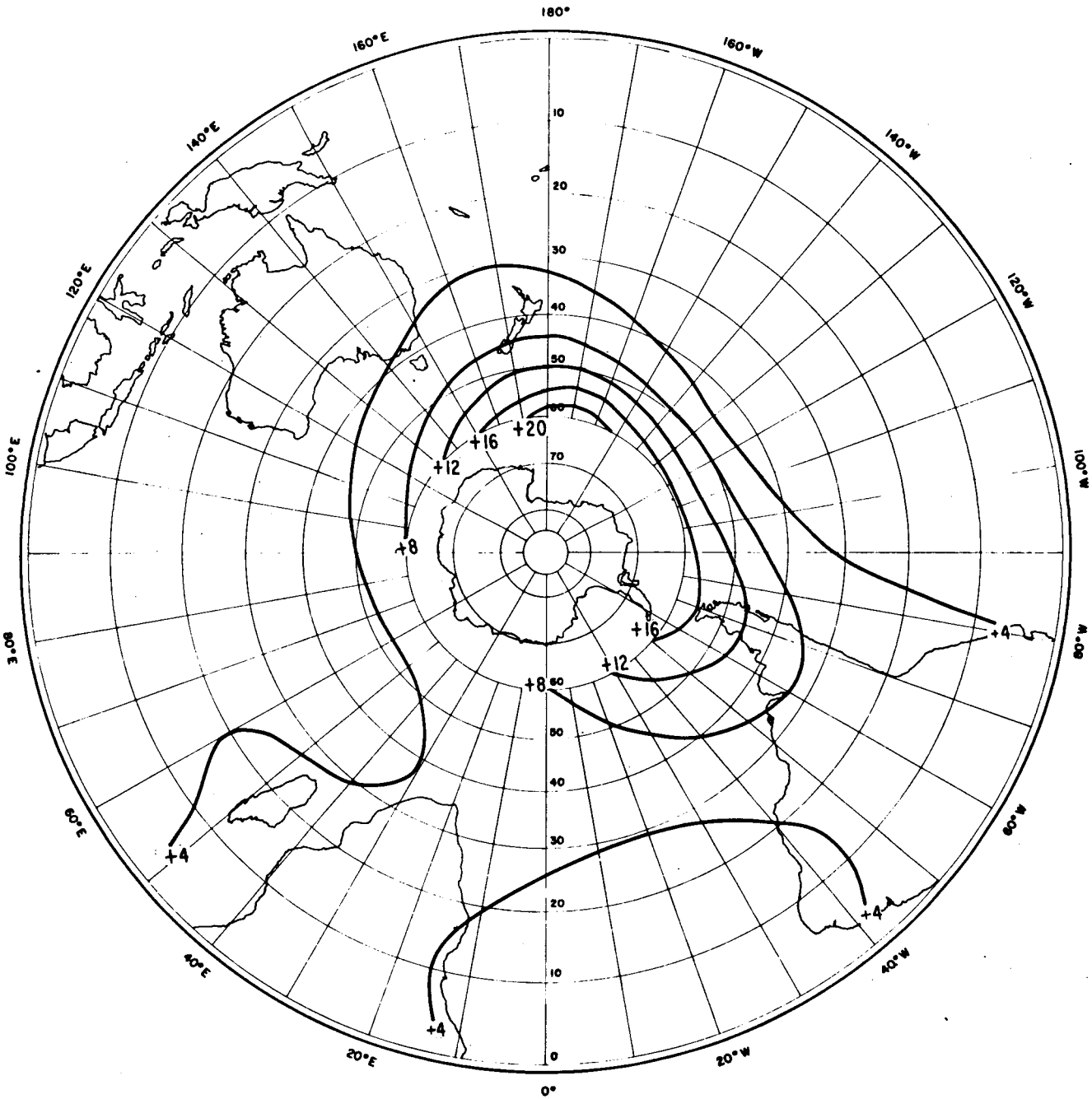

Figure 14 The 15-micron temperature change from 14 October to 21 November 1963 in the southern hemisphere taken from 10-day mean maps

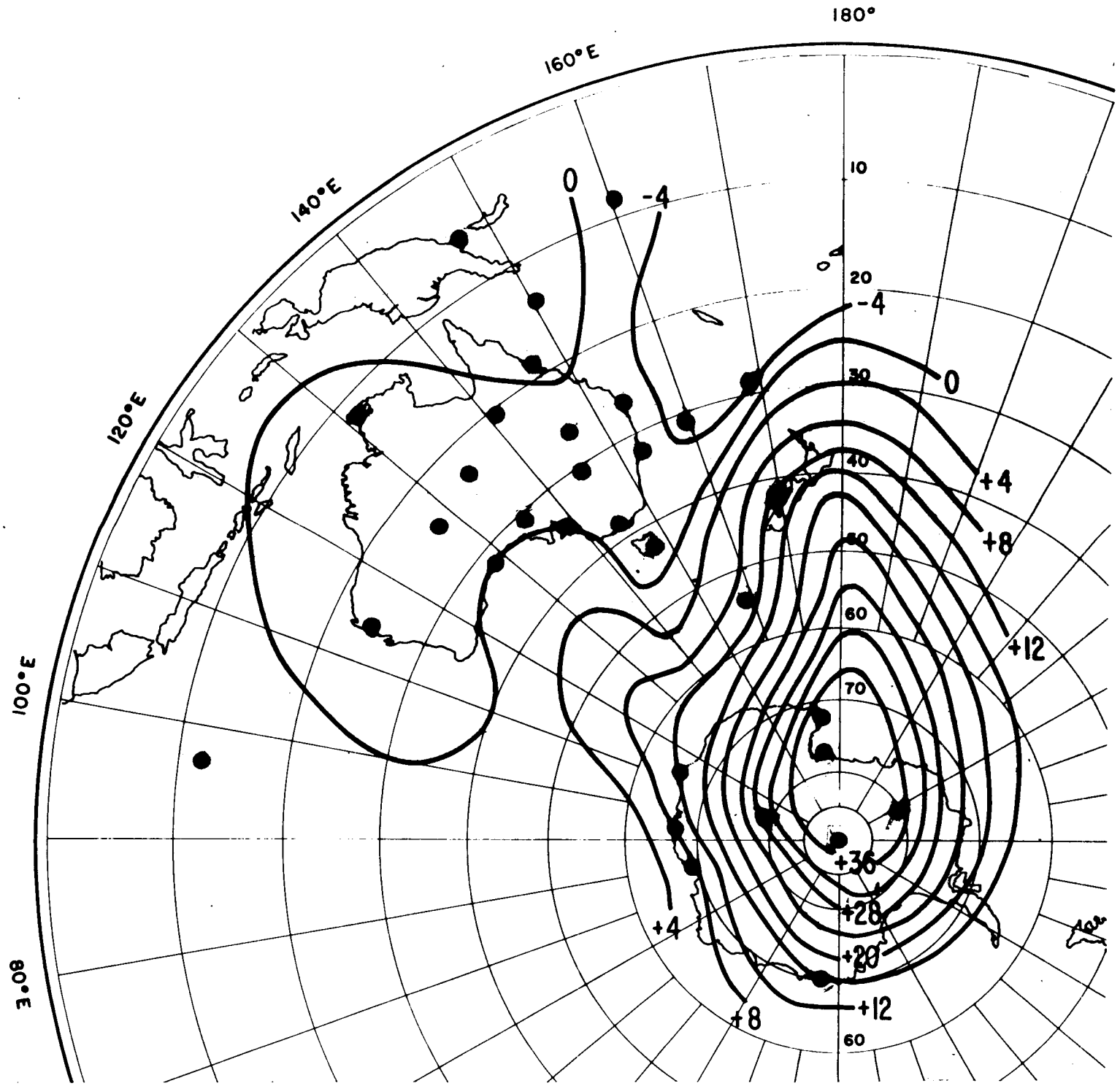

Figure 15 The 70 mb temperature changes from 15 October to 20 November 1963 for available stations in the southern hemisphere

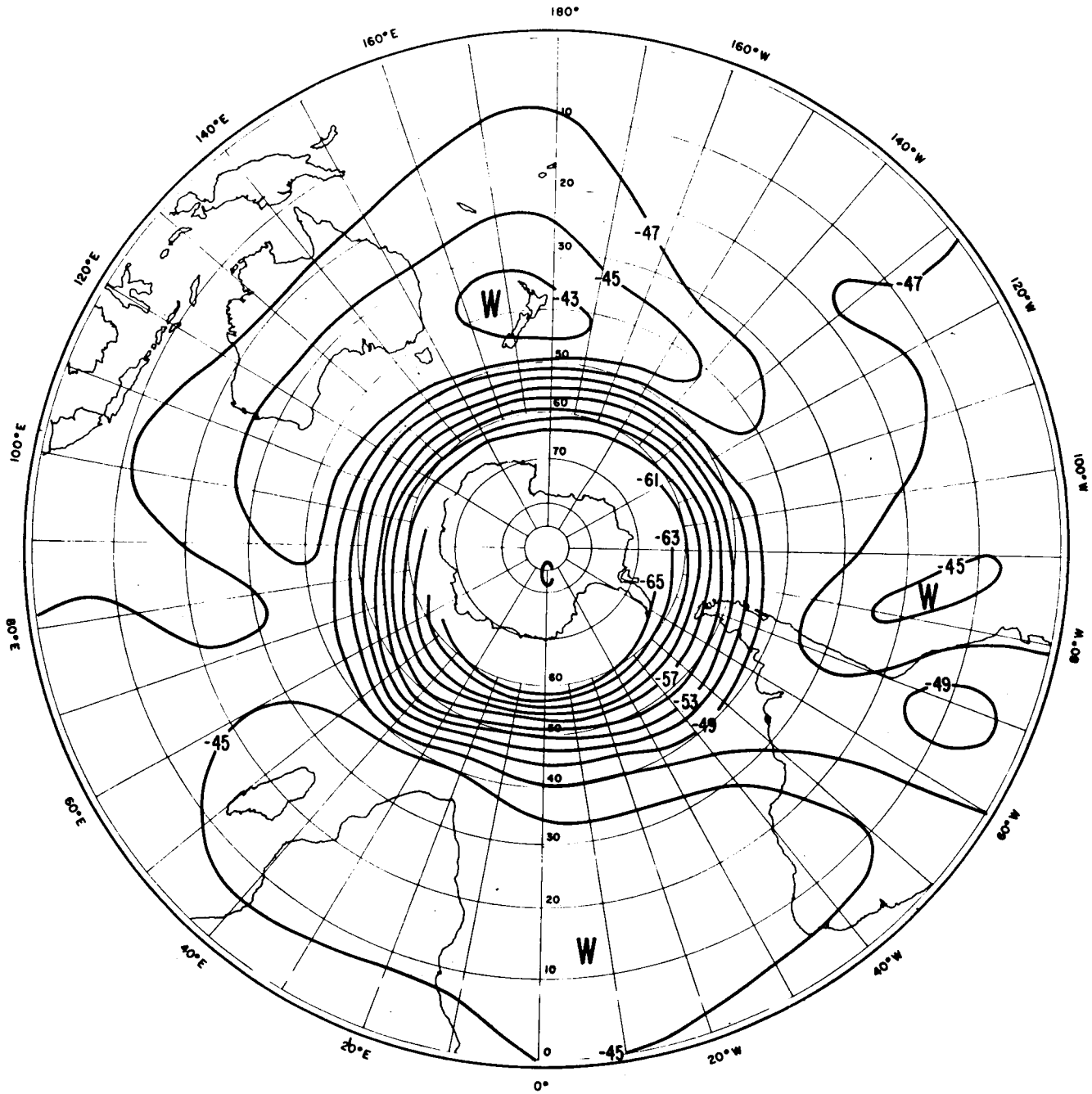

Figure 16 10-day mean 15-micron temperatures for 9-18 August 1963

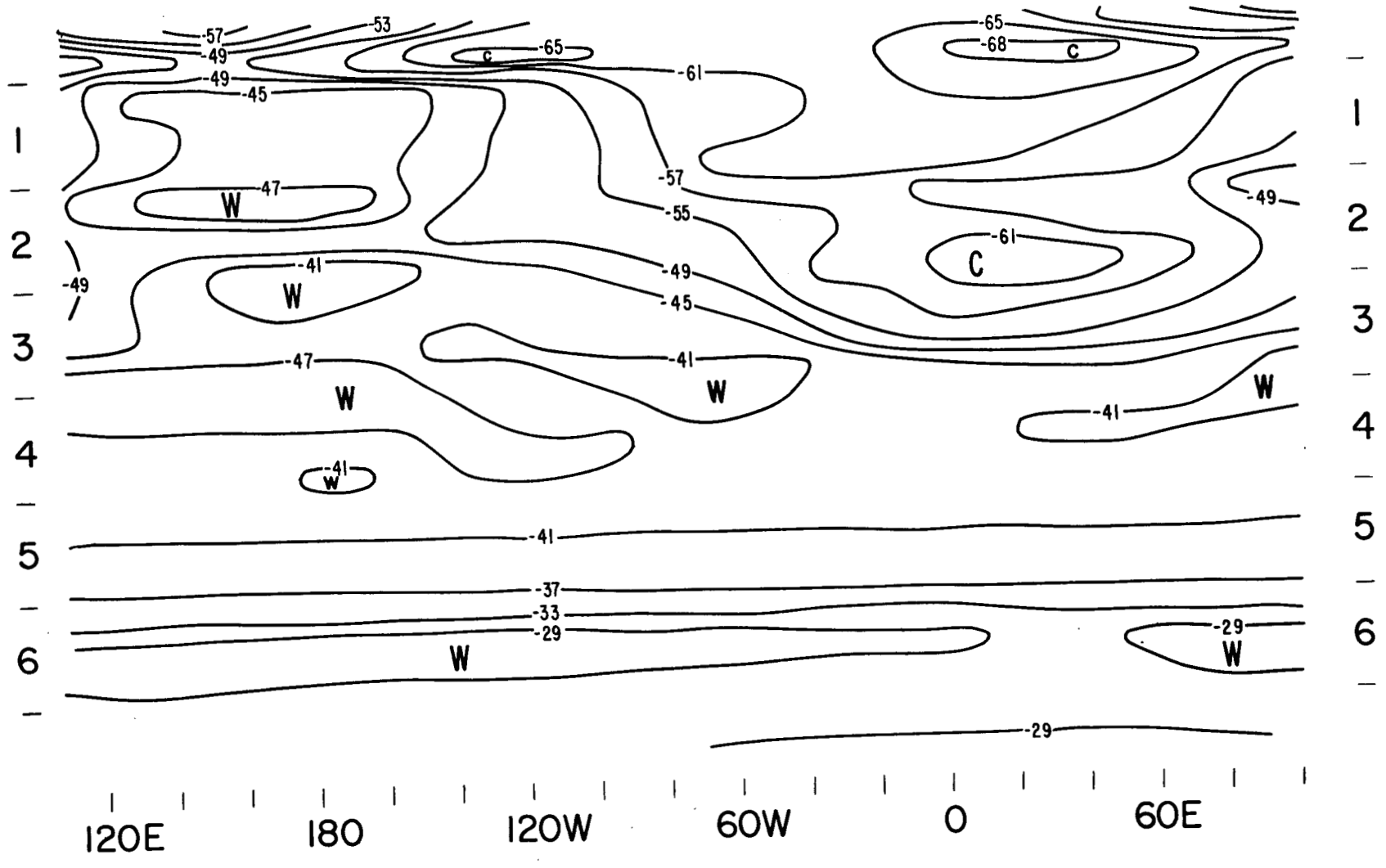

Figure 17 Temporal variation of 15-micron 10-day mean temperature along 60N (January-June, 1964)

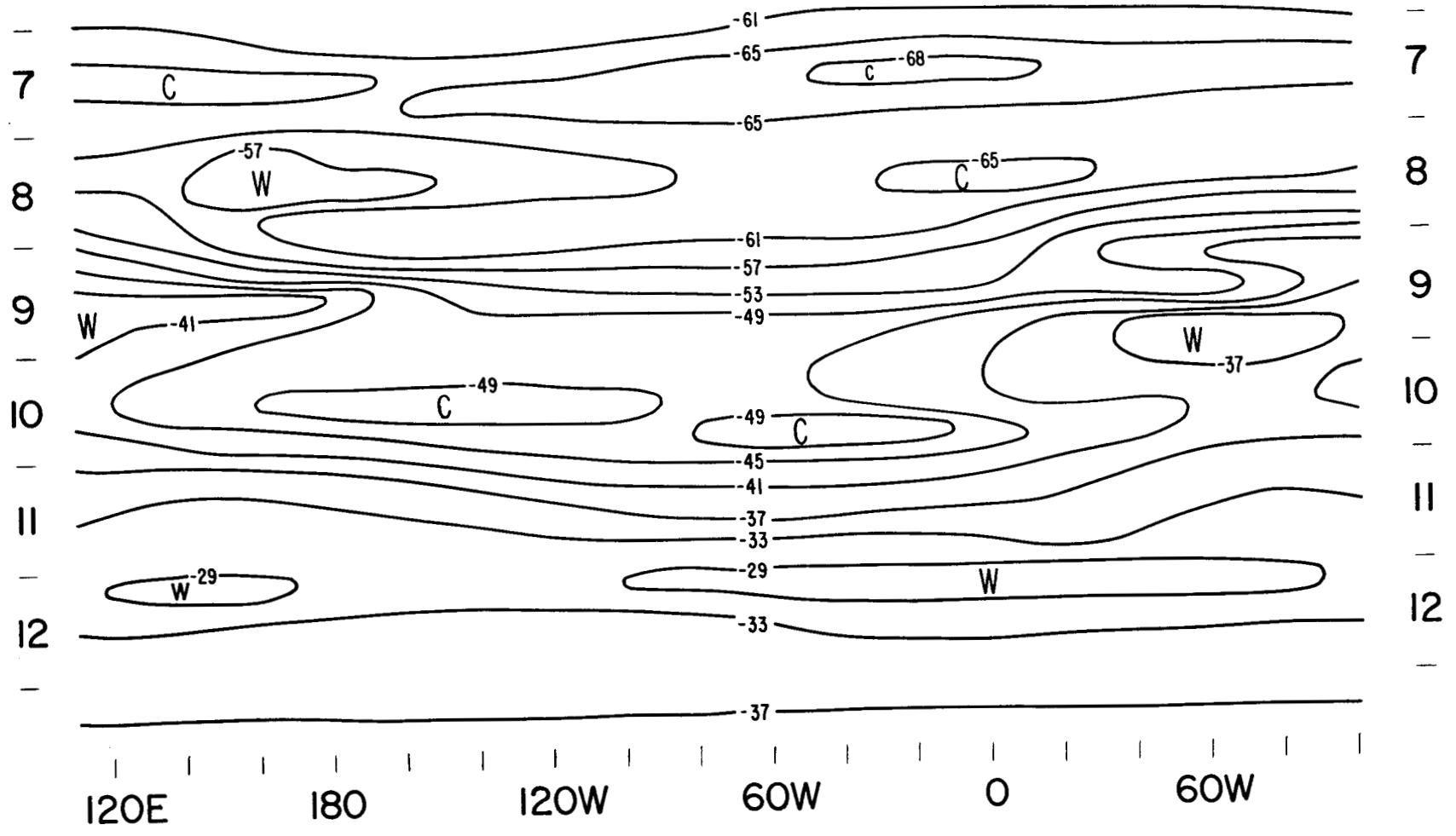

Figure 18 Temporal variation of 15-micron 10-day mean temperature along 60S (July-December, 1963)